Epindolidiones-Versatile and Stable Hydrogen-Bonded Pigments for Organic Field-Effect Transistors and Light-Emitting Diodes

Advanced Functional Materials

Epindolidiones - versatile and stable hydrogen-bonded pigments for organic field-effect transistors and light-emitting diodes

--Manuscript Draft--

Manuscript Number:	
Full Title:	Epindolidiones - versatile and stable hydrogen-bonded pigments for organic field-effect transistors and light-emitting diodes
Article Type:	Full Paper
Section/Category:	
Keywords:	hydrogen-bonded organic semiconductors; organic pigments; indigoids; organic field-effect transistors; organic electronics
Corresponding Author:	Eric Daniel Glowacki Johannes Kepler University AUSTRIA
Additional Information:	
Question	**Response**
Please submit a plain text version of your cover letter here. **If you are submitting a revision of your manuscript, please do not overwrite your original cover letter. There is an opportunity for you to provide your responses to the reviewers later; please do not add them here**.	To the Advanced Functional Materials editorial staff, Please find enclosed our original submission entitled “Epindolidiones – versatile and stable hydrogen-bonded pigments for organic field-effect transistors and light-emitting diodes” to be considered for publication in Advanced Functional Materials. In this work we explore the semiconducting properties of epindolidiones, a highly-stable organic hydrogen-bonded pigment family. The class of materials known as H-bonded pigments has not been explored until very recently in the field of organic electronics as they are perceived as having inferior π-conjugation – they were simply not expected to work as semiconductors. Nevertheless, such materials are in ubiquitous use industrially, renowned for stability, non-toxicity, and low cost. In this paper we explore electronic transport in three epindolidiones, correlating it with their crystal structure which we have been successful in measuring, and their optical properties. We evaluate the extraordinary operational stability of field-effect transistor devices, which can operate stably in various ionic solutions in a pH range from 3-10 without any passivation. We discuss in detail also epindolidione synthesis, as well as preparation and properties of latent pigment derivatives which allow solution processing. We think this work will stimulate more exploration into using low-cost industrial pigments as viable electronic materials. Additionally, the impressive stability in aqueous ionic environments is of substantial interest for the growing field of deploying organic semiconductors in biochemical applications. We thank you, the editorial team, and referees in advance for consideration of our work.
Corresponding Author Secondary Information:	
Corresponding Author's Institution:	Johannes Kepler University
Corresponding Author's Secondary Institution:	
First Author:	Eric Daniel Glowacki
First Author Secondary Information:	
Order of Authors:	Eric Daniel Glowacki
	Giuseppe Romanazzi
	Cigdem Yumusak
	Halime Coskun

	Uwe Monkowius
	Gundula Voss
	Max Burian
	Rainer Lechner
	Nicola Demetri
	Günther Redhammer
	Nevsal Sunger
	Gian Paolo Suranna
	Serdar Sariciftci
Order of Authors Secondary Information:	
Abstract:	Hydrogen-bonded pigments are remarkably stable organic solids with high-crystal lattice energy. Here we report on a lesser-known family of compounds, the epindolidiones, which we have found demonstrate electronic transport with extraordinary stability, even in highly-demanding aqueous environments. Hole mobilities in the range 0.05 - 1 cm2/Vs can be achieved, with lower electron mobilities of up to 0.1 cm2/Vs. To help understand charge transport in epindolidiones, X-ray diffraction was used to solve the crystal structure of 2,8-difluoroepindolidione and 2,8-dichloroepindolidione. Both derivatives crystallize with a linear-chain H-bonding lattice featuring two-dimensional π-π stacking. Powder diffraction indicates that the unsubstituted epindolidione has very similar crystallinity. All types of epindolidiones measured here display strong low-energy optical emission originating from excimeric states, which coexists with higher-energy fluorescence. This can be exploited in light-emitting diodes, which show the same hybrid singlet and low-energy excimer electroluminescence. We fabricated low-voltage FETs with epindolidione which operate reliably under repeated cyclic tests in ionic solutions within the pH range 3-10 without degradation. Finally, in order to overcome the insolubility of epindolidiones in organic solvents, we devised a procedure to allow solution-processing via the introduction of suitable thermolabile solubilizing groups. This work shows the versatile potential of epindolidione pigments for electronics applications.

WILEY-VCH

DOI: 10.1002/ ((please add manuscript number))

Full Paper

Epindolidiones – versatile and stable hydrogen-bonded pigments for organic field-effect transistors and light-emitting diodes

E. D. Głowacki, G. Romanazzi, C. Yumusak, H. Coskun, U. Monkowius, G. Voss, M. Burian, R. T. Lechner, N. Demetri, G. J. Redhammer, N. Sünger, G. P. Suranna, N. S. Sariciftci*

[*] Dr. E.D. Głowacki, Dr. C. Yumusak, H. Coskun, Dr. G. Voss, Prof. N.S. Sariciftci
Linz Institute for Organic Solar Cells (LIOS)
Johannes Kepler University, A-4040 Linz Austria
E-mail: eric_daniel.glowacki@jku.at
Dr. G. Romanazzi, Prof. G. P. Suranna
Dipartimento di Ingegneria Civile, Ambientale, del Territorio, Edile e di Chimica (DICATECh), Politecnico di Bari, Via Orabona 4, 70125, Bari, Italy
Dr. C. Yumusak
Department of Physics, Faculty of Arts and Sciences, Yildiz Technical University, Davutpasa Campus, Esenler, 34210 Istanbul, Turkey
Prof. U. Monkowius
Institute of Inorganic Chemistry
Johannes Kepler University, A-4040 Linz Austria
M. Burian, Prof. R. T. Lechner
Institute of Physics, Montanuniversitaet Leoben, Franz-Josef-Strasse 18, 8700 Leoben, Austria
N. Demetri
Elettra – Sincrotrone Trieste, S.S. 14 Km 163.5 in Area Science Park, 34149 Basovizza, Trieste, Italy
Dr. G. J. Redhammer,
Materialwissenschaften und Physik, Abteilung für Mineralogie, Paris-Lodron Universität Salzburg, Hellabrunner Str. 34, 5020 Salzburg, Austria
N. Sünger
Solar Energy Institute, Ege University, Izmir, Turkey

Keywords: hydrogen-bonded organic semiconductors, organic pigments, indigoids, organic field-effect transistors, organic electronics

Abstract: Hydrogen-bonded pigments are remarkably stable high-crystal lattice energy organic solids. Here we report on a lesser-known family of compounds, the epindolidiones, which we have found demonstrate electronic transport with extraordinary stability, even in highly-demanding aqueous environments. Hole mobilities in the range 0.05 – 1 cm^2/Vs can be achieved, with lower electron mobilities of up to 0.1 cm^2/Vs. To help understand charge transport in epindolidiones, X-ray diffraction was used to solve the crystal structure of 2,8-difluoroepindolidione and 2,8-dichloroepindolidione. Both derivatives crystallize with a linear-chain H-bonding lattice featuring two-dimensional π-π stacking. Powder diffraction

indicates that the unsubstituted epindolidione has very similar crystallinity. All types of epindolidiones measured here display strong low-energy optical emission originating from excimeric states, which coexists with higher-energy fluorescence. This can be exploited in light-emitting diodes, which show the same hybrid singlet and low-energy excimer electroluminescence. We fabricated low-voltage FETs with epindolidione which operate reliably under repeated cyclic tests in different ionic solutions within the pH range 3-10 without degradation. Finally, in order to overcome the insolubility of epindolidiones in organic solvents, we devised a chemical procedure to allow solution-processing via the introduction of suitable thermolabile solubilizing groups. This work shows the versatile potential of epindolidione pigments for electronics applications.

1. Introduction

Hydrogen-bonded organic pigments are a class of materials familiar from applications in the colorant industry, where they find widespread use as materials for robust outdoor paints, cosmetics, and printing inks.[1,2] Indigo, a natural product, is the oldest and still most widely produced organic dye and pigment (**Figure 1**).[3] The intermolecular –NH···O= hydrogen bonding that characterizes indigo is exploited in most of the synthetic hydrogen-bonded pigments as well. This class of materials has proven to be nontoxic and safe for humans, and is considered safer than even several classes of food dyes.[4] Recently, we have found that indigo[5] and some of its derivatives[6,7] demonstrate ambipolar transport in organic field-effect transistors (OFETs), with mobility ranging from 0.01 – 0.4 cm^2/Vs. We then reported on quinacridone, a common industrial colorant perhaps best known as constituting the magenta printer pigment, as an ambipolar semiconductor with mobility in the 0.01-0.1 cm^2/Vs range (Figure 1).[8] Quinacridone also demonstrated the formation of low-energy luminescent species, attributed to charge transfer excitons, which led to a low effective exciton binding energy and promising photovoltaic behavior.[9] Alongside quinacridone, we evaluated its 4-ring analog epindolidione (Figure 1). Epindolidione demonstrated promising behavior in OFETs, providing hole mobility as high as 1.5 cm^2/Vs with excellent stability in air.[8] Indigo, epindolidione, and quinacridone are all examples of hydrogen-bonded pigments where interplay between intermolecular H-bonds and π-π stacking interactions lead to strong intermolecular interactions and high crystal lattice energy solids.[1,2,10] A substantial bathochromic shift in absorption accompanied by increased oscillator strength occurs from dilute solutions to the solid state (Figure 1b). Intramolecular H-bonding in indigo results in ultrafast proton transfer in the excited state, quenching luminescence.[11] Quinacridone and

epindolidione, in contrast, are highly luminescent in solution. Epindolidione is a structural isomer of indigo, however photophysically it is very different – it is highly luminescent, even in the solid state, and is yellow/orange, instead of blue. Additionally, as we report herein, it crystallizes with a very different structure than indigo. In this work we follow up on the epindolidione class of compounds, detailing synthetic preparation and characterization of epindolidiones, their crystalline structure, optical and electrochemical properties, and results from OFETs and electroluminescent devices. Finally, we revisit the issue of epindolidione OFET stability, showing also that such devices can operate with excellent stability even in aqueous environments within a pH range from 3-10.

2. Results and Discussion

2.1. Synthesis and characterization of epindolidiones

The synthetic approach followed to obtain the epindolidiones: *dibenzo[b,g][1,5]naphthyridine-6,12(5H,11H)-dione* (Epi), *2,8-difluorodibenzo[b,g][1,5]naphthyridine-6,12(5H,11H)-dione* (2F-Epi), *2,8-dichlorodibenzo[b,g][1,5]naphthyridine-6,12(5H,11H)-dione* (2Cl-Epi) is detailed in **Scheme 1** and follows the procedure reported by Jaffe and Matrick,[12] although the suggestions by Kemp *et al.*[13] concerning the preparation of intermediates 1-3 have also been taken into account. Dimethyl dihydroxyfumarate (1) reacts rapidly with aniline, or *p*-fluoroaniline or *p*-cloroaniline, under hydrochloric acid catalysis to give precipitation of dimethyl bis(arylamino)maleates 2a-c in high yields. The *Z* geometry of 2a-c was confirmed by ^{1}H-NMR spectra as well as by the presence of a very strong FT-IR absorption at 1570 cm^{-1} ascribable to the olefinic stretching of maleate. In boiling Dowtherm^{TM} A and under high dilution, maleates 2a-c isomerize into dimethyl bis(arylamino)fumarates, which then undergo the expected Conrad-Limpach cyclization to give the corresponding carbomethoxyquinolones 3a-c in high yields. Eventually, ring closure of 3a-c to give Epi, 2F-Epi, and 2Cl-Epi respectively was carried out at 150°C in polyphosphoric acid (PPA) under high dilution conditions. After hydrolysis of the PPA solution, epindolidiones Epi, 2F-Epi, 2Cl-Epi precipitated as greenish yellow to yellow powders; overall yields with respect to the initial amount of dihydroxyfumaric acid were 51.1, 57.8, and 61.1% respectively. The target molecules Epi, 2F-Epi, 2Cl-Epi are very sparingly soluble in common organic solvents, however, their structures could be confirmed by solution ^{1}H-NMR in deuterated dimethyl sulfoxide (DMSO-d_6) or deuterosulfuric acid (D_2SO_4). Their purity was proven by CHN

elemental analysis. This synthetic procedure can in principle be applied to a wide range of substituted anilines, many of which are well-known commercially-available materials. Thus many epindolidione derivatives can be prepared from cheap aniline building blocks.

2.2 Solubilization of epindolidione by *t*-butoxycarbonylation (tBOC protection).

The very poor solubility in common organic solvents of Epi limits its thin-film processability to vacuum-evaporation. It also precludes further synthetic chemical derivatization. Thus, the latent pigment approach was pursued in order to obtain a soluble material suitable for solution-processing or further chemical manipulation. Applied to epindolidione, this approach consists of the reaction of the N-H group with di-*tert*-butyl dicarbonate $(tBOC)_2O$, a well-known protecting group for amine functions. As a result, the H-bond network is transiently disrupted, leading to a solubility improvement of orders of magnitude and thereby allowing solution processing. The tBOC groups are subsequently removed by simple heating (or by acid treatment) with the release of gaseous CO_2 and isobutene. This procedure was introduced for insoluble industrial pigments like diketopyrrolopyrroles and quinacridones by researchers at the *Ciba-Geigy* company.[14,15]

Contrary to other H-bonded pigments, which can readily be functionalized with tBOC according to several simple procedures[14–16], the t-butoxycarbonylation of Epi proved to be quite a demanding task. After several attempts, we were able to find the best protocol (**Scheme 2**) in terms of yields and reaction time. A stoichiometric amount of 4-dimethylaminopyridine (DMAP) and a large excess of $(tBOC)_2O$ were necessary to obtain, after flash chromatography, di-tBOC Epi and mono-tBOC Epi. The persistence of a significant amount of mono-tBOC Epi in the reaction mixture is likely caused by the stability of the *enol* tautomeric form of this compound. ^{1}H NMR of mono-tBOC Epi in chloroform confirms that the hydroxyquinoline tautomer is dominant in equilibrium in solution, explaining why the reaction with a second tBOC group is impeded.

The tBOC derivatives proved to be, as expected, highly soluble: the solubility of di-tBOC Epi reaches concentrations up to ~25 mg/ml in chloroform. Solution processing of films using di-tBOC Epi is described in detail in section 2.7.

2.3 Crystal structure

An important step in understanding the charge transport in H-bonded epindolidione pigments is to evaluate the solid state structure of such materials. Diffraction-quality single crystals of hydrogen-bonded pigments can typically be grown using physical vapor transport

recrystallization. Establishing the crystal structure of the closely-related quinacridone family of pigments presented a challenge to crystallographers for many years, as growing defect-free crystals of suitable size required considerable trial-and-error optimization. Details concerning this long-term effort were the subject of three review articles on quinacridone crystallography.[17–19] We encountered similar problems, and were unable despite many attempts to grow suitable crystals of Epi using vapor or solution-based methods. These crystals were either very small, in the < 10 µm range, or had multiple twinning defects. However, successful crystal growth was achieved with 2F-Epi and 2Cl-Epi. The materials were first purified twice via temperature-gradient sublimation and then loaded into an alumina crucible and heated to 330-350 °C in a borosilicate glass tube under a 2 L/min flow of dry N_2 gas. Over the course of 3-5 days, large single crystals grew in the downstream 110-130 °C zone of the glass tube. 2Cl-Epi crystals could be measured using Cu K_α radiation on a standard Bruker diffractometer. The smaller 2F-Epi crystals were measured using 0.7 Å synchrotron radiation. Both materials crystallize in the same fashion: Projections of the crystal structure of 2Cl-Epi are shown in **Figure 2**. The two halogenated derivatives crystallize with a linear-chain H-bonding lattice featuring two-dimensional π-π stacking, very similar to the quinacridone α_I phase.[19] Molecules are H-bonded to two neighbors, forming infinite linear chains which are parallel to each other. These linear chains are π-π stacked on top of each other in a brick-wall pattern. The NH···O= H-bond length is very short: 2F-Epi, (2Cl-Epi, in parenthesis); 2.05 (2.06) Å, very close to that found in the quinacridone α_I phase (2.01 Å). Indigos, for comparison, have H-bond lengths of 2.1 – 2.8 Å. Intermolecular distances for stacking interactions are 3.9 Å (3.69 Å) along a, and 6.2 Å (5.97 Å) along b. As in the case of other H-bonded pigment semiconductors, it is concluded that charge transport primarily occurs perpendicular to the H-bonding plane, along the two π-stacking directions. The short H-bond lengths and close stacking interactions are together accountable for the high crystal lattice energy of epindolidione pigments, as observed by thermogravimetric (TGA) analysis (**Figure 3**). All three epindolidione pigments were found to sublime cleanly with no charred residue, with sublimation temperatures > 405 °C. This high sublimation point is indicative of strong intermolecular interactions and high crystal lattice energy. As a reference example, tetracene has an analogous structure and similar molecular weight, but sublimes at 280 °C under the same experimental conditions.[8] We were not successful to grow diffraction-quality crystals of the tBOC-derivatives epindolidiones, however in the loss of isobutene and CO_2 is found to occur at 190 °C, followed by sublimation at the same temperature as the measured

unsubstituted epindolidione. This confirms the successful regeneration of H-bonded epindolidione following thermal deprotection.

2.4 Optical Properties

Epindolidiones described in the patent literature are pigments with yellow or orange color. All three derivatives described here are yellow powders. The solubility of the epindolidiones is very poor in organic solvents, but they can be dissolved at concentrations < 200 µM in polar aprotic solvents such as DMSO and DMF after heating and sonication. **Figure** a shows the extinction coefficients of Epi, 2F-Epi, 2Cl-Epi dissolved in DMSO. A typical vibronic progression is clear for all compounds. Epindolidiones are isomers of indigo, and contain a very similar cross-conjugated system. For indigo, the cross-conjugated arrangement of electron-rich NH groups with the electron-withdrawing carbonyl functions produces the so-called H-chromophore, which supports a low-energy charge-transfer type absorption.[7,20] Our observations on the three epindolidione derivatives appear to support the hypothesis that they are indeed H-chromophore systems as well. If epindolidiones are treated as an H-chromophore system like the cross-conjugated indigos, the presence of a π-electron donor *para* to the nitrogen (donor component in the H-chromophore) should shift absorption bathochromically by virtue of increasing the donor ability of the NH groups. This is consistent with the observation that the halogenated compounds have a ~10 nm bathochromic shift in absorption onset compared to the unsubstituted Epi. Photoluminescence and excitation spectra for Epi, 2F-Epi, and 2Cl-Epi are shown in panels b, c, and d, respectively, of Figure . While the halogenated derivatives show a typical Franck-Condon mirror-image luminescence spectrum, for unsubstituted Epi the highest energy luminescence peak is weak compared with the next lower-energy PL peak. This is reflected also in the excitation spectrum. The origin of this effect is unclear. The PL yields of epindolidiones in solution are high,[21] much higher than in the case of indigos. Indigos undergo a photoinduced intramolecular proton transfer, leading to a tautomerization reaction followed by relaxation, leading to overall efficient radiationless internal conversion and very weak photoluminescence ($\varphi_f = 1\times10^{-3}$).[7,11] This tautomerization mechanism is blocked in the case of epindolidione by their fused-ring structure. Therefore epindolidiones can be regarded as H-chromophoric molecules without a proton-mediated relaxation pathway and thus high luminescence.

In order to better understand the optical properties of epindolidiones, we carried out DFT calculations with a 6-311+g(d,p) basis set. The optimized ground state geometries and charge isodensity plots for the HOMO and LUMO orbitals of the three Epi derivatives are

shown in **Figure** . The HOMO orbitals are concentrated on an extended conjugated segment consisting of the two nitrogen atoms bridged by the central C=C group, while the LUMO orbitals are shifted to the carbonyl functions and C-C units. This is consistent with the H-chromophore model.[20,22] Indeed, the calculated plots for epindolidione are very similar to those of indigo itself.[23] The addition of halogens *para* to the nitrogen groups is thus expected, according to the H-chromophore model, to influence primarily the HOMO. This is seen in the isodensity plots, where indeed charge density is localized over the halogens in the HOMO but not the LUMO orbitals. According to DFT, both HOMO and LUMO energies are lower than in unsubstituted Epi, leading to smaller band gap, which is observed experimentally as well. Vacuum-evaporated thin films of the three Epi derivatives have absorption onsets bathochromically-shifted by about 50 nm relative to solutions (**Figure**). This is characteristic of H-bonded pigments, where close lattice packing leads to a large degree of intermolecular electronic interaction.[2] Moreover, the effect of supramolecular mesomerism, where sharing of the proton via H-bonding markedly shifts the electronic properties of such molecules, has also been proposed as an explanation for large bathochromic shifts in H-bonded pigments.[18] The PL of evaporated films features a Stokes-shifted peak in the green, and several peaks far to the red, at 625, 690, and 780 nm for all derivatives. The red-shift for these emissive features is too large to be explained by vibronic replicas, also their oscillator strength is relatively high. Two explanations for these peaks can be put forward: either they originate from extrinsic defect states in the solid-state films, or they are excimeric species. Defect states in such films may arise from impurities, states at grain boundaries between the crystallites, or interfaces between polymorphic forms. It should be stressed that the presence of the low-energy luminescence peaks, as well as their position and relative intensity, was found to be highly reproducible over a wide range of sample preparation conditions. The luminescence features were found to be invariant over evaporation rates of < 0.1 – 6 Å/s, substrate temperatures of 25 – 140 °C, post-deposition annealing, as well as solvent annealing procedures which are known to induce rearrangements in H-bonded pigments.[24] Based on the lack of effect of processing conditions, and the high purity of the sublimation-purified material, we propose that extrinsic defect state luminescence is not likely responsible for the low-energy emission, but rather true excimeric species. This hypothesis is further supported by fluorescence microscopy of single crystals (Figure S2), where both green and red emission is found to originate from the bulk of the crystals. Both the singlet and excimeric PL features were found to be robust and resistant to degradation under conditions of aging the samples in air, or exposure to water.

2.5 Electrochemical properties

Cyclic voltammetry was carried out on 80 nm thick films of epindolidiones evaporated on ITO-coated glass functioning as the working electrode. A platinum foil was used as the counter electrode and an Ag/AgCl wire as the pseudo-reference electrode. All three derivatives demonstrated reduction and oxidation behavior (**Figure**). Evaluating the reversibility is complicated by the fact that both the reduced and oxidized forms of the epindolidiones are highly-soluble in the polar electrolyte solution. Thus, the smaller currents corresponding to the reverse redox processes are caused, in large part, by the substantially diminished quantity of analyte on/near the working electrode. Reduction appears to be quasi-reversible for all three derivatives, while oxidation not so. Epi showed an oxidation onset at 1200 mV (HOMO = -5.6 eV), 2Cl-Epi at 1350 mV (HOMO = -5.7 eV), and 2F-Epi at 1800mV (HOMO = -5.8 eV). The oxidation potential, not surprisingly, scales with the electronegativity of the halogen substituents. The reduction potential, however, did not display a similar trend. All three derivatives show a reduction peak with an onset of -1500 mV vs. Ag/AgCl, corresponding to a LUMO level of approx. -2.9 eV versus vacuum. This is easy to rationalize due to the 2,8 positions of the halogens on the substituted epindolidione molecules according to the H-chromophore model, as discussed in section 2.3. As the halogens are *para* to the NH groups, they have an inductive withdrawing effect on the electron-rich NH part of the molecule, thereby affecting the oxidation potential markedly. However the halogens have no inductive effect on the carbonyl functional groups of the molecule, which are responsible of the electron-accepting properties of these molecules. From an electrochemical point of view, epindolidiones can be both reduced quasi-reversibly, and oxidized, but they are wide band gap materials with relatively high potentials needed to achieve reduction or oxidation.

2.6 Organic field-effect transistors (OFETs)

2.6.1. Measurement of OFETs

OFETs were fabricated with the three Epi derivatives using a 32 nm-thick anodically-grown AlO_x passivated with a layer of linear-chain hydrocarbon $C_{44}H_{90}$ (tetratetracontane, or TTC) as described in earlier works.[7] This composite gate dielectric has a C_{0d} of ~40 nF/cm^2. Mobility was calculated from the saturation regime.[25] Top source-drain contacts were evaporated through a shadow mask, giving channel dimensions of W = 2 mm, L = 60 µm. Gold source-drain contacts afforded p-type operation, while aluminum contacts gave n-type

behavior. The transfer curve of a typical p-type epindolidione device is shown in **Figure** a. Average devices gave mobilities of 0.2 cm^2/Vs, though champion devices had mobilities of around ~1 cm^2/Vs. Smaller channel lengths can be correlated to higher mobilities, as we previously demonstrated for Epi FETs.[8] With aluminum contacts, Epi showed n-type behavior (Figure b), albeit with a significantly lower mobility of 2×10^{-3} cm^2/Vs. Based on the LUMO level of -2.9 eV calculated from cyclic voltammetry, it is likely that a significant barrier to electron injection exists and thus contact resistance limits n-type operation. In the case of 2-F Epi (Figure c) and 2-Cl Epi (Figure d), only n-type mobility could be observed. The deep HOMO values resulting from the strong electron affinity of the halogen functional groups, as evidenced from cyclic voltammetry, cause a substantial hole injection barrier. While the electron mobility of 2-Cl Epi was relatively low, 2×10^{-3} cm^2/Vs, 2F-Epi showed an impressive average electron mobility of 0.1 cm^2/Vs. From these results it is clear that by simple derivitization of the epindolidione core, both n- and p-type behavior can be obtained.

FETs with Epi as the active layer were measured in air over 250 days, with no statistical decline in mobility whatsoever. This correlates with our earlier work,[8] where samples fabricated as part of that study still operate at the same level after ~ 2 years.

2.6.2 Stability in aqueous environment

Motivated by possible applications of stable FETs for bioelectronics applications[26], we evaluated the stability of Epi FETs in various aqueous environments. To operate under water, high capacitance gate dielectrics must be used to keep operating voltages in the range of 1-2 V. We utilized anodic aluminum oxide prepared with an anodization voltage of 5V, giving an AlO_x layer with a thickness of ~ 8 nm. This layer was then modified by application of an n-octadecyl phosphonic acid self-assembled monolayer, giving a C_{0d} of approx. 350 nF/cm^2.[27] Devices with top source-drain contacts of gold were used without any passivation layer, thus the Epi/Au surface layer was in direct contact with the water environment. A poly(dimethylsiloxane) rubber block was used to confine the electrolyte over the entire transistor active area, with a volume of 40 µL of fluid over the FET device. We utilized a test sequence to evaluate OFET performance in a pH range from 3-10 and in the presence of a wide range of various ionic species. Transfer characteristics were measured over 60 cycles in each of a series of different aqueous environments sequentially using a scan rate of 150 mV/s (**Figure 9**): 18 MΩ high-purity water, pH 7 acetate buffer solution, a pH 7.6 phosphate buffer solution, a pH 4 acetate buffer solution, a pH 3 HCl solution, and a pH 10 NaOH solution. Between measurements the devices were rinsed with deionized water. A total of 360 cycles

were measured in this test, plus 10 cycles for dry samples before and after the assay. Devices measured in air with a V_{SD} = -0.5V exhibited a saturation current of around 100 nA at a V_G = -2.5V and an on/off ratio of ~10^3. After 360 cycles in the different aqueous environments the same performance was found, as can be seen comparing the black trace in the first panel of Figure 8 and the blue trace in the final panel. All the "wet" environments featured an off current about 10 times higher than in the dry state, due to ionic current between source and drain. This current is not dependent on pH, and thus this off-current increase cannot be attributed to doping of the Epi layer but indeed to electrochemical currents in the electrolyte solution. The on current and threshold voltage of the Epi transistors remained constant while cycling under the different electrolyte environments. Previous studies have shown OFETs stable over cycling in pH 7 water[28], however to our knowledge no study has shown stability in a pH range as wide as that of the present study. This result demonstrating excellent stability in quite demanding aqueous environments suggests that epindolidiones can be highly effective active materials in devices for bioelectronics.

2.7 Organic light-emitting diodes (OLEDs)

Diodes with the structure ITO/PEDOT:PSS/Epi/Al were fabricated in order to evaluate the electroluminescence spectra of the different epindolidione derivatives. J-V characteristics are shown in **Figure 10a**. The electroluminescence spectra (Figure 10b) of each of the derivatives featured the same S_1-S_0 transitions and excimeric peaks at higher wavelengths as the PL spectra. The combination of green and red electroluminescence led to an overall yellow/orange-colored emission. The CIE 193 chromaticity coordinates were: Epi, (0.60, 0.40), 2F-Epi, (0.59, 0.38), 2-Cl Epi, (0.35,0.62). The electroluminescent performance of each material was comparable, with relatively low brightness of 10-25 cd/m^2. Experimenting with different growth parameters such as substrate temperature (from 30 °C up to 120 °C) and deposition rate (either slow growth of 0.1Å/s and 5-6 Å/s) demonstrated no changes in either the brightness of the devices or the relative intensities of the singlet vs. excimer emissions, again providing evidence as to intrinsic excimeric species being responsible for the low-energy emission as opposed to extrinsic trap states. To evaluate the air stability of Epi OLEDs, we fabricated devices with the structure ITO/PEDOT:PSS/Epi/PEIE/Au, where PEIE = poly(ethylene imine, ethoxylated), a modification layer providing good electron-injection ability.[29] The diodes were found to emit while operating in air with a brightness of ~15 cd/m^2 for a period of 3 weeks. The low electroluminescence of these devices is a problem that may be mitigated by optimizing electron and hole injection layers to provide balanced injection of

charges to increase radiative recombination in the epindolidione layer. Excimer-emitting materials are nevertheless an interesting concept to achieve polychromic emission from a single semiconducting material, and have been suggested as a possible route to achieving practical white-light emitting OLEDs.[30]

2.8 Solubilized epindolidiones and solution processing using the latent pigment route

As described in section 2.2, epindolidiones can be functionalized with solubilizing thermolabile tBOC protecting groups. The double-substituted di-tBOC Epi shows solubility up to about 25 mg/ml in solvents like chloroform, toluene, and chlorobenzene. The mono-tBOC derivative, however, was considerably less soluble in these solvents (up to 1 mg/ml max), though still far more soluble than unfunctionalized Epi. Uniform films of di-tBOC Epi could be obtained by spin-casting. Heating these films at 185 °C for 5 minutes was sufficient to achieve complete deprotection and transformation of the pale yellow di-tBOC Epi films into darker yellow films of Epi (**Figure 11**a). The optical properties of the films, *i.e.* absorbance and photoluminescence, were identical to evaporated films. Unfortunately, repeated attempts to fabricate transistors using this method, on a variety of gate dielectric materials, yielded very poor transport. The origin of this problem is not clear, though previous studies on hydrogen-bonded pigments like indigo concluded that orientation of molecules with π-π stacking parallel to the substrate was critical, and this favorable growth is achieved via evaporation on hydrophobic substrates. Diodes with the structure ITO/PEDOT:PSS/Epi/Al could be fabricated however, yielding performance indistinguishable from evaporated diodes. To obtain a pinhole-free film, a 10mg/ml solution of di-tBOC Epi in chloroform was spin cast following heating to 185°C for 5 minutes, and then a second coating followed by heating. The diodes functioned as OLEDs with the same singlet/excimer emission as the vacuum-processed devices. Absorbance spectra in dilute solution of mono-tBOC- and di-tBOC-Epi are shown in comparison with Epi in Figure 11b, with the corresponding photoluminescence spectra in Figure 11c. The absorbance spectra in solution are very similar to one another, while in the luminescence spectra there is a marked red shift in emission proceeding from unsubstituted Epi, mono-tBOC Epi, to di-tBOC Epi. The increased conjugation length across the molecule provided by the carbonyls on the tBOC groups is likely the cause for this red shift. In absorbance spectra of films (Figure 11d), the situation is different than in solution. The unsubstituted H-bonded form of Epi has a ~ 75 nm red shift in absorbance compared to the tBOC derivatives and a significantly higher oscillator

strength. This underscores the importance of intermolecular H-bonding for the optical properties of epindolidione in the solid state.

3. Conclusions

We have evaluated epindolidione and two halogenated derivatives in terms of their applications as organic semiconductors. Epindolidiones are a class of robust H-bonded organic pigments with a simple synthetic preparation which starts from the well-known aniline class of compounds. From a photophysical perspective, they are H-chromophore systems like the closely-related indigos, however with a hypsochromic absorption relative to indigo and a bright luminescence. A distinctive feature of the epindolidiones is strong excimeric emission – thus a yellow material absorbing in the blue can give strong yellow/red photoluminescence. Electrochemically, epindolidiones can be oxidized and quasi-reversibly reduced, albeit with a substantial band gap. This translates to both electron and hole transport in transistor devices with the appropriate choice of source-drain contact metal. Low-voltage FETs fabricated with epindolidione were found to have extraordinary stability in a wide range of electrolyte solutions, wherein devices operated reliably with no degradation over hundreds of cycles. To our knowledge, no other organic semiconducting materials have demonstrated stability in such a wide range (pH 3-10 was measured here with no degradation). Due to their luminescence and ambipolarity, we found that epindolidiones can be used in electroluminescent devices, where the distinctive combination of higher-energy singlet and lower-energy excimeric electroluminescence is observed. Finally, we have presented a technique of introducing transient protection groups (tBOC) in order to disrupt H-bonding and yield a soluble dye form of epindolidiones. This allows solution-processing techniques as well as potentially enables further chemical derivatization. This work demonstrates the potential of this highly-stable pigment as a versatile organic semiconducting material. Research in industry on organic pigments has developed, over the past century, a range of highly-stable heterocyclic systems synthesized from low-cost precursors. This work suggests that more exploration of this materials class as functional materials for modern technological applications is warranted.

4. Experimental section

Details on synthetic procedures and materials characterization data are presented in the supplementary information. Evaporation of thin films of the Epi compounds was done using a

custom-built organic evaporation system from *Vaksis R&D and Engineering*, allowing precise rate control and substrate heating. For UV-Vis spectra, a Perkin-Elmer Lambda 950 spectrometer was used. Spectroscopic-grade DMSO was used for all optical measurements in solutions. PL spectra were recorded on a photomultiplier tube-equipped double-grating input and output fluorometer manufactured by PhotoMed. Electrochemical measurements were carried out in a dry N_2 environment using a Pt foil as counter electrode, an Ag/AgCl wire as a pseudo-reference electrode, and ~80nm films of the Epi compounds vacuum evaporated on ITO as the working electrode. The supporting electrolyte was 0.1 M *n*-tetrabutylammonium hexafluorophosphate in dry acetonitrile. Frontier orbital levels were calculated according to: $E_{HOMO} = -(E_{[onset, ox. vs. NHE]} + 4.75)(eV)$; $E_{LUMO} = -(E_{[onset, red. vs. NHE]} + 4.75)(eV)$. Measurements were calibrated against ferrocene/ferrocenium redox couple (Fc/Fc^+). The values of the Fc/Fc^+ vs NHE and NHE vs. vacuum level used in this work were 0.64 and −4.75 V, respectively.[31] ITO glass slides used for electrochemistry and diode fabrication were cleaned sequentially with acetone, isopropanol, detergent, and DI water, and finally treated with O_2 plasma. Glass slides for OFET fabrication were prepared in the same way. Aluminum/aluminum Oxide/TTC gate structures were prepared according to reported methods.[32,33]For low-voltage OFETs optimized for operation in aqueous environments, ultrathin aluminum oxide layers (~ 8 nm) were prepared using the potentiostatic method[27,34] with a 5 V anodization voltage, treated for 1 minute in oxygen plasma to active the surface, and passivated with n-octadeceylphosphonic acid (C18-PA) according to reported methods,[35] by immersing for 12 hours in a C18-PA 5 mM solution in isopropanol. The samples were rinsed with isopropanol and water and then heated *in vacuo* at 110 °C prior to evaporation of the epindolidione semiconductor layer. OFET properties were measured using an Agilent B1500A parameter analyzer in ambient air environment. The quantitative electroluminescence spectra were measured using a Photo Research Spectrascan PR-655. IV measurements were carried out with a Keithley 2600 source measurement unit.

[CCDC 1013233 and 1013474 contain the supplementary crystallographic data for this paper. These data can be obtained free of charge from The Cambridge Crystallographic Data Centre via www.ccdc.cam.ac.uk/data_request/cif.]

Supporting Information

Supporting Information is available from the Wiley Online Library or from the author.

Acknowledgements

We are grateful for support by the Austrian Science Foundation, FWF, within the Wittgenstein Prize of N. S. Sariciftci Solare Energie Umwandlung Z222-N19 and the Translational Research Project TRP 294-N19 “Indigo: From ancient dye to modern high-performance organic electronics circuits”. Italian MIUR – PON project “Molecular Nanotechnologies for Health and Environment-MAAT” (PON02_005633316357 – CUP B31C12001230005) is also acknowledged.

Received: ((will be filled in by the editorial staff))
Revised: ((will be filled in by the editorial staff))
Published online: ((will be filled in by the editorial staff))

[1] H. Zollinger, *Color Chemistry. Syntheses, Properties and Applications of Organic Dyes and Pigments*; 3rd ed.; Wiley-VCH: Weinheim, 2003; Vol. 43.
[2] *High Performance Pigments*; Faulkner, E. B.; Schwartz, R. J., Eds.; 2nd ed.; Wiley-VCH: Weinheim, 2009.
[3] M. Seefelder, *Indigo in culture, science, and technology*; 2nd ed.; ecomed: Landsberg, Germany, 1994.
[4] K. Hunger, *Rev. Prog. Color. Relat. Top.* **2005**, *35*, 76.
[5] M. Irimia-Vladu, E. D. Głowacki, P. A. Troshin, G. Schwabegger, L. Leonat, D. K. Susarova, O. Krystal, M. Ullah, Y. Kanbur, M. A. Bodea, V. F. Razumov, H. Sitter, S. Bauer, N. S. Sariciftci, *Adv. Mater.* **2012**, *24*, 375.
[6] E. D. Głowacki, L. Leonat, G. Voss, M.-A. Bodea, Z. Bozkurt, A. M. Ramil, M. Irimia-Vladu, S. Bauer, N. S. Sariciftci, *AIP Adv.* **2011**, *1*, 042132.
[7] E. D. Głowacki, G. Voss, N. S. Sariciftci, *Adv. Mater.* **2013**, *25*, 6783.
[8] E. D. Głowacki, M. Irimia-Vladu, M. Kaltenbrunner, J. Gąsiorowski, M. S. White, U. Monkowius, G. Romanazzi, G. P. Suranna, P. Mastrorilli, T. Sekitani, S. Bauer, T. Someya, L. Torsi, N. S. Sariciftci, *Adv. Mater.* **2013**, *25*, 1563.
[9] E. D. Głowacki, L. Leonat, M. Irimia-Vladu, R. Schwo□diauer, M. Ullah, H. Sitter, S. Bauer, N. Serdar Sariciftci, *Appl. Phys. Lett.* **2012**, *101*, 023305.
[10] W. Herbst, K. Hunger, *Industrial Organic Pigments*; 3rd ed.; Wiley-VCH: Weinheim, 2004.
[11] S. Yamazaki, L. Sobolewski, W. Domcke, *Phys. Chem. Chem. Phys.* **2011**, *13*, 1618.
[12] E. E. Jaffe, *Surf. coatings Int. JOCCA, J. Oil Colour Chem. Assoc.* **1992**, *75*, 24.
[13] D. S. Kemp, B. R. Bowen, C. C. Muendel, *J. Org. Chem.* **1990**, *55*, 4650.
[14] U. Schaedeli, J. S. Zambounis, A. Iqbal, Z. Hao, H. Dubas, **1993** EP 0654711
[15] J. S. Zambounis, Z. Hao, A. Iqbal, *Nature* **1997**, *388*, 131.
[16] E. D. Glowacki, G. Voss, K. Demirak, M. Havlicek, N. Sunger, A. C. Okur, U. Monkowius, J. Gasiorowski, L. Leonat, N. S. Sariciftci, *Chem. Commun.* **2013**, *49*, 6063
[17] G. Lincke, *Dyes Pigments* **2000**, *44*, 101.
[18] G. Lincke, *Dyes Pigments* **2002**, *52*, 169.
[19] E. F. Paulus, F. J. J. Leusen, M. U. Schmidt, *CrystEngComm* **2007**, *9*, 131.
[20] W. Lüttke, H. Hermann, M. Klessinger, *Angew. Chemie Int Ed.* **1966**, *5*, 598.
[21] W. Tuer, PhD Dissertation, Epindolidione , Epindoline und lineare sowie trigonale Imidazolderivate Neue Materialien mit interessanten Fluoreszenzeigenschaften, Ludwig-Maximilians-University Munich, **2001**.
[22] H. Sieghold, PhD dissertation: Synthesen und Spektrosckopisches verhalten von heteroanalogen carbonylkindigo-farbstoffen, University of Göttingen, **1973**.

[23] A. Amat, F. Rosi, C. Miliani, A. Sgamellotti, S. Fantacci, *J. Mol. Struct.* **2011**, *993*, 43.
[24] J. Mizuguchi, *Berichte der Bunsengesellschaft für Phys. Chemie* **1993**, *97*, 684.
[25] D. Braga, G. Horowitz, *Adv. Mater.* **2009**, *21*, 1473.
[26] L. Torsi, M. Magliulo, K. Manoli, G. Palazzo, *Chem. Soc. Rev.* **2013**.
[27] A. I. Mardare, M. Kaltenbrunner, N. S. Sariciftci, S. Bauer, A. W. Hassel, *Phys. Status Solidi* **2012**, *209*, 813.
[28] M. E. Roberts, S. C. B. Mannsfeld, N. Queraltó, C. Reese, J. Locklin, W. Knoll, Z. Bao, *Proc. Natl. Acad. Sci. U. S. A.* **2008**, *105*, 12134.
[29] Y. Zhou, C. Fuentes-Hernandez, J. Shim, J. Meyer, A. J. Giordano, H. Li, P. Winget, T. Papadopoulos, H. Cheun, J. Kim, M. Fenoll, A. Dindar, W. Haske, E. Najafabadi, T. M. Khan, H. Sojoudi, S. Barlow, S. Graham, J.-L. Bredas, S. R. Marder, A. Kahn, B. Kippelen, *Science* **2012**, *336*, 327.
[30] G. M. Farinola, R. Ragni, *Chem. Soc. Rev.* **2011**, *40*, 3467.
[31] C. M. Cardona, W. Li, A. E. Kaifer, D. Stockdale, G. C. Bazan, *Adv. Mater.* **2011**, *23*, 2367.
[32] M. Kraus, S. Richler, A. Opitz, W. Bru□tting, S. Haas, T. Hasegawa, A. Hinderhofer, F. Schreiber, *J. Appl. Phys.* **2010**, *107*, 094503.
[33] E. D. Głowacki, M. Irimia-Vladu, S. Bauer, N. S. Sariciftci, *J. Mater. Chem. B* **2013**, *1*, 3742.
[34] M. M. Lohrengel, *Mater. Sci. Eng. R* **1993**, *11*, 243.
[35] M. Kaltenbrunner, T. Sekitani, J. Reeder, T. Yokota, K. Kuribara, T. Tokuhara, M. Drack, R. Schwödiauer, I. Graz, S. Bauer-Gogonea, S. Bauer, T. Someya, *Nature* **2013**, *499*, 458.

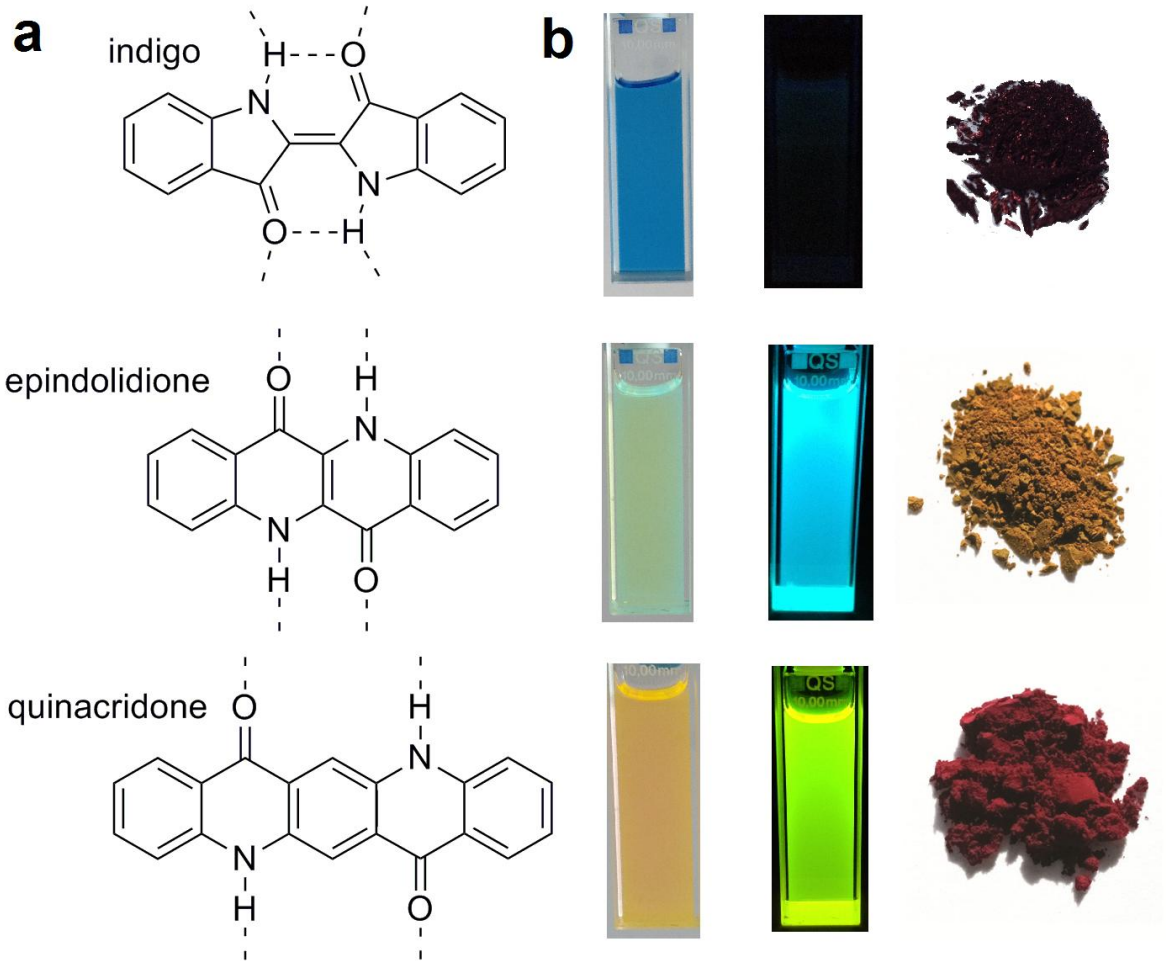

Figure 1. a) Molecular structures of indigo, its isomer epindolidione, and quinacridone. Dashed lines indicate hydrogen-bonding. b) 0.1 mM solutions of each material in DMSO, with photoluminescence excited at 365 nm. While epindolidione and quinacridone are highly-emissive, indigo has very low luminescence quantum yield. The powders of the three pigments are shown on the right, where the bathochromically-shifted absorption and tinctorial strength are visible.

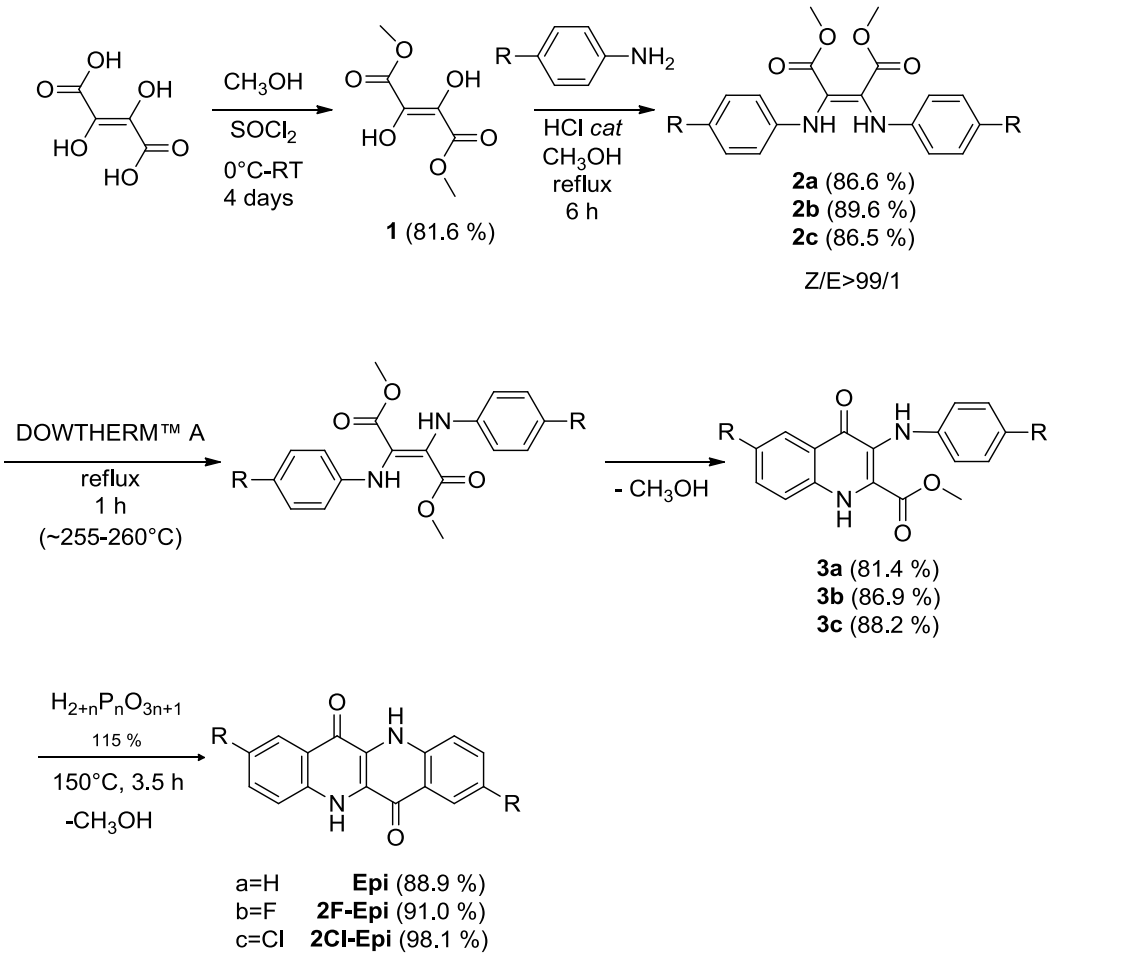

Scheme 1. Synthetic procedure for preparing epindolidiones from *para*-substituted anilines.

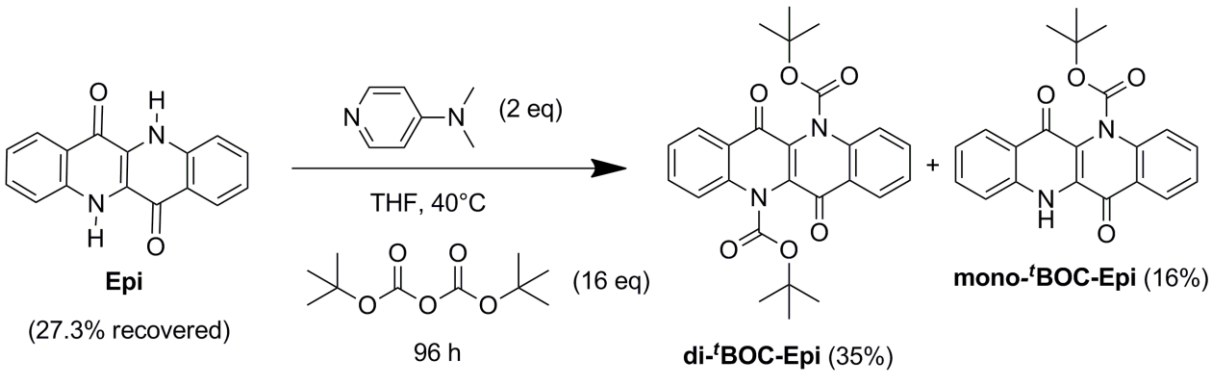

Scheme 2. Protection reaction to obtain tBOC-functionalized epindolidione.

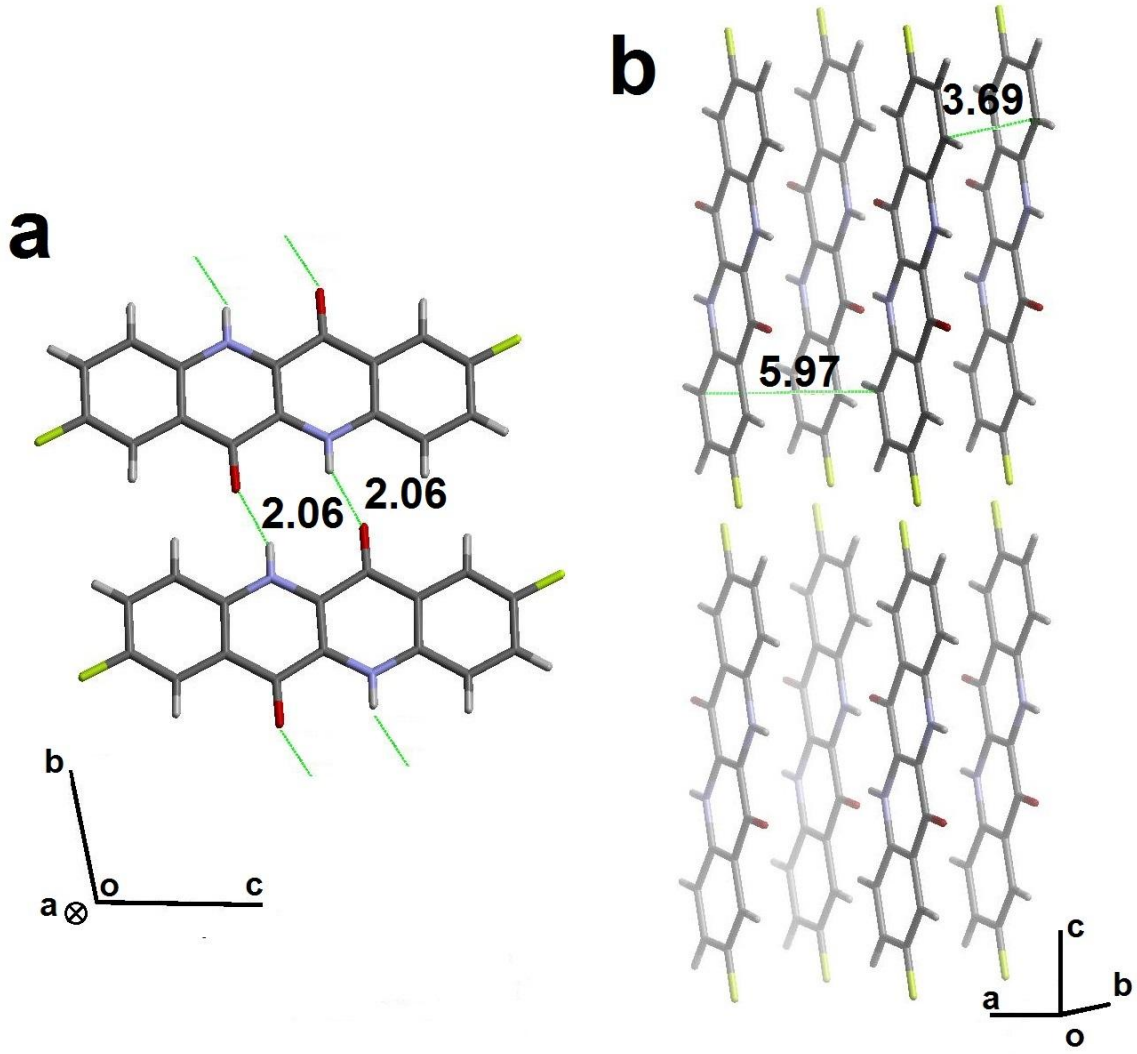

Figure 2. Crystal structure of 2F-Epi obtained from single-crystal X-ray diffraction using synchrotron radiation with a wavelength of 0.7 Å. a) View down the a axis showing the propagation of linear H-bonded chains of molecules. b) View down the b-axis with π-π stacking interactions (with intermolecular distances shown in green). The measured crystal structure of 2Cl-Epi is qualitatively identical to this one.

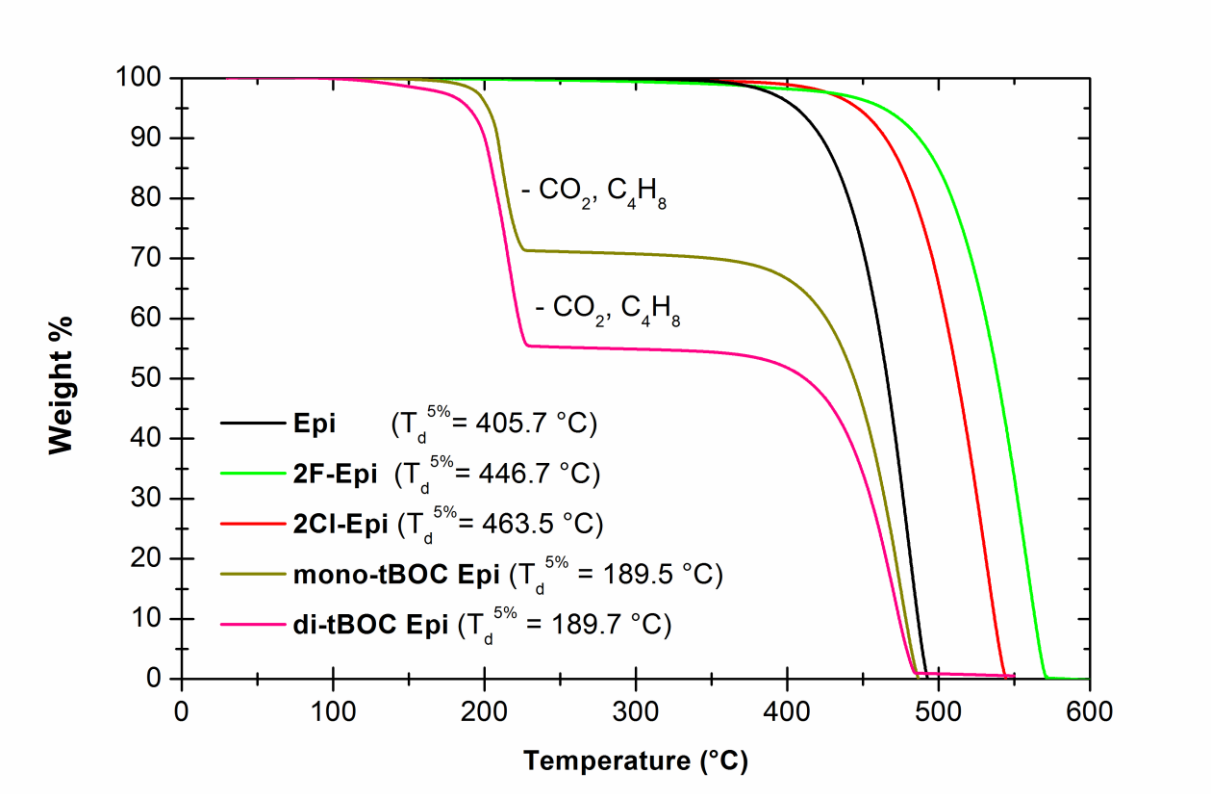

Figure 3. TGA scans for the three epindolidiones and the mono- and di-tBOC epindolidione. In the latter case the loss of carbon dioxide and isobutene is clearly visible.

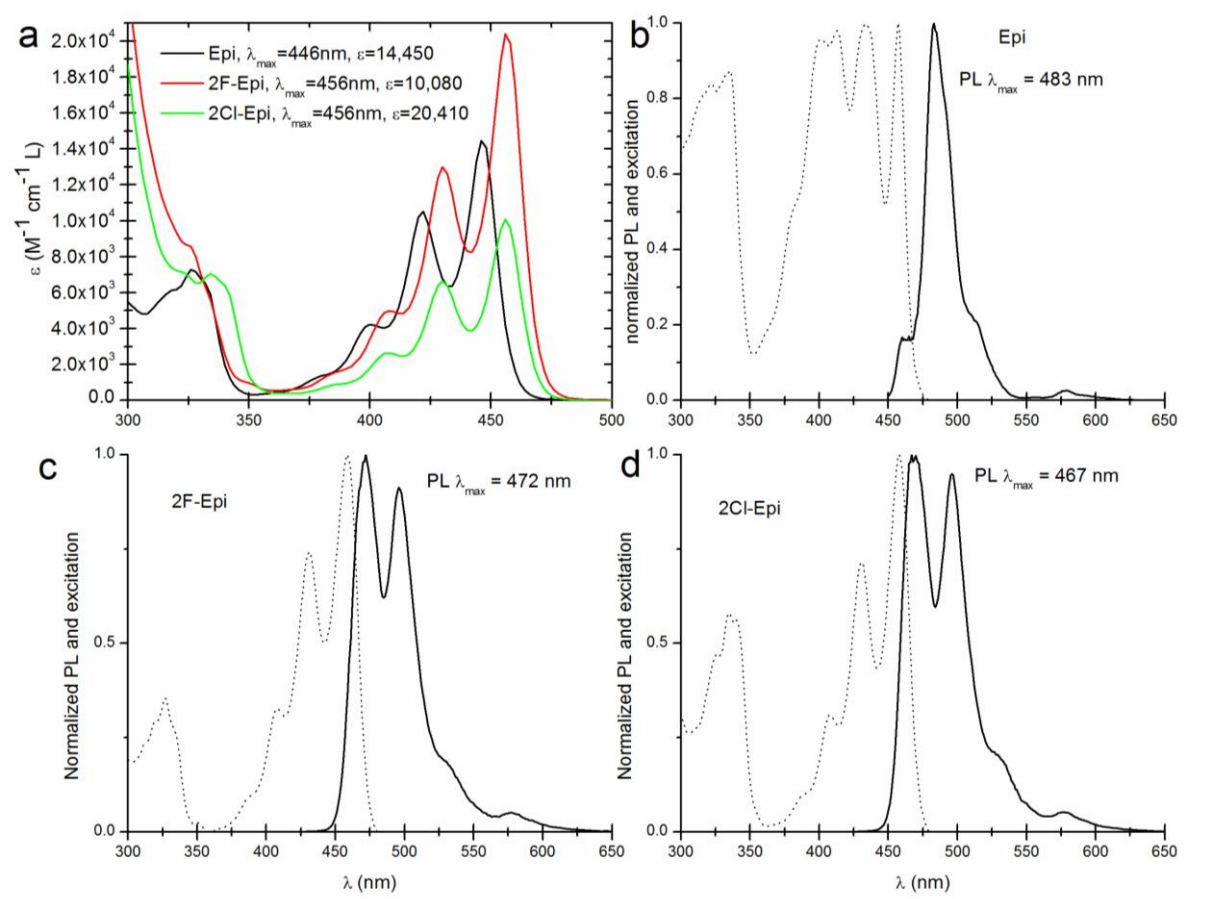

Figure 4. a) UV-Vis absorption and photoluminescence of 0.1 mM solutions of the three epindolidiones in DMSO. b) PL and excitation spectra for 0.1 mM Epi in DMSO. c) PL and excitation spectra for 0.1 mM 2F-Epi in DMSO. c) PL and excitation spectra for 0.1 mM 2Cl-Epi

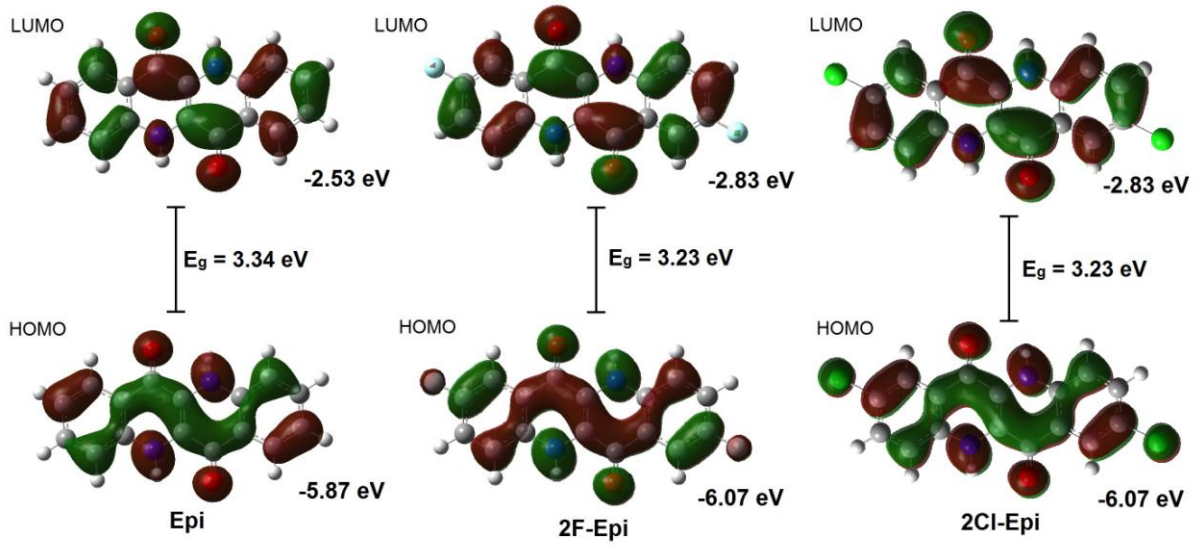

Figure 5. Optimized ground-state geometries and frontier orbital energies of epindolidione and the two halogenated derivatives.

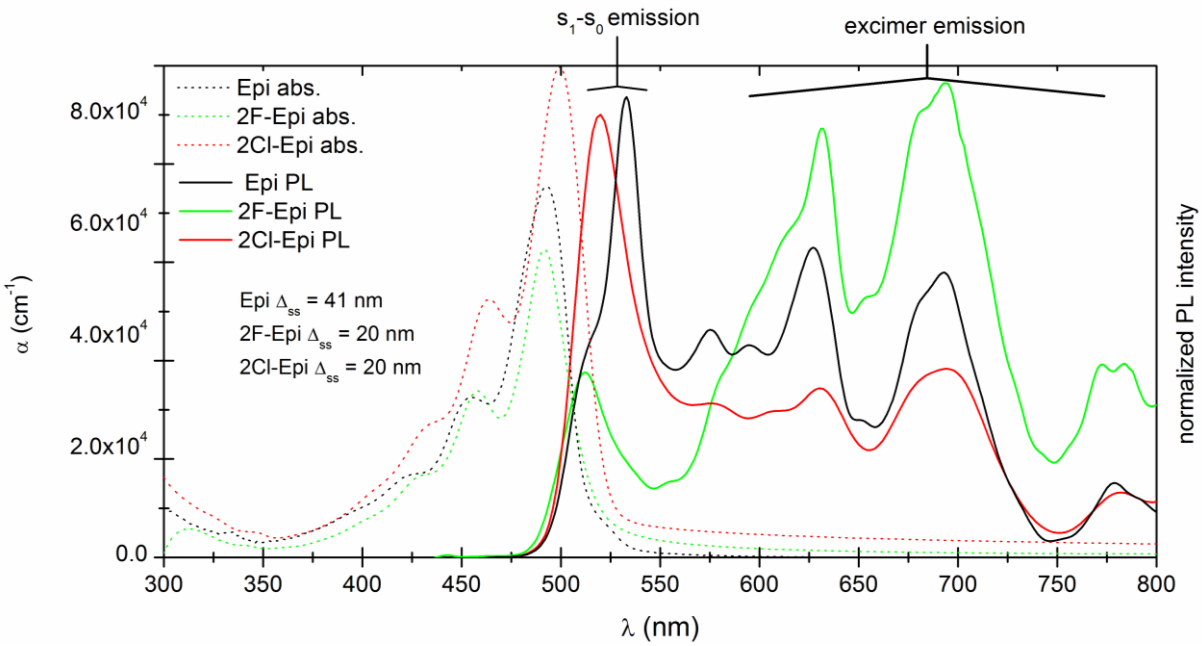

Figure 6. UV-Vis absorption and photoluminescence of the three epindolidiones deposited on glass slides.

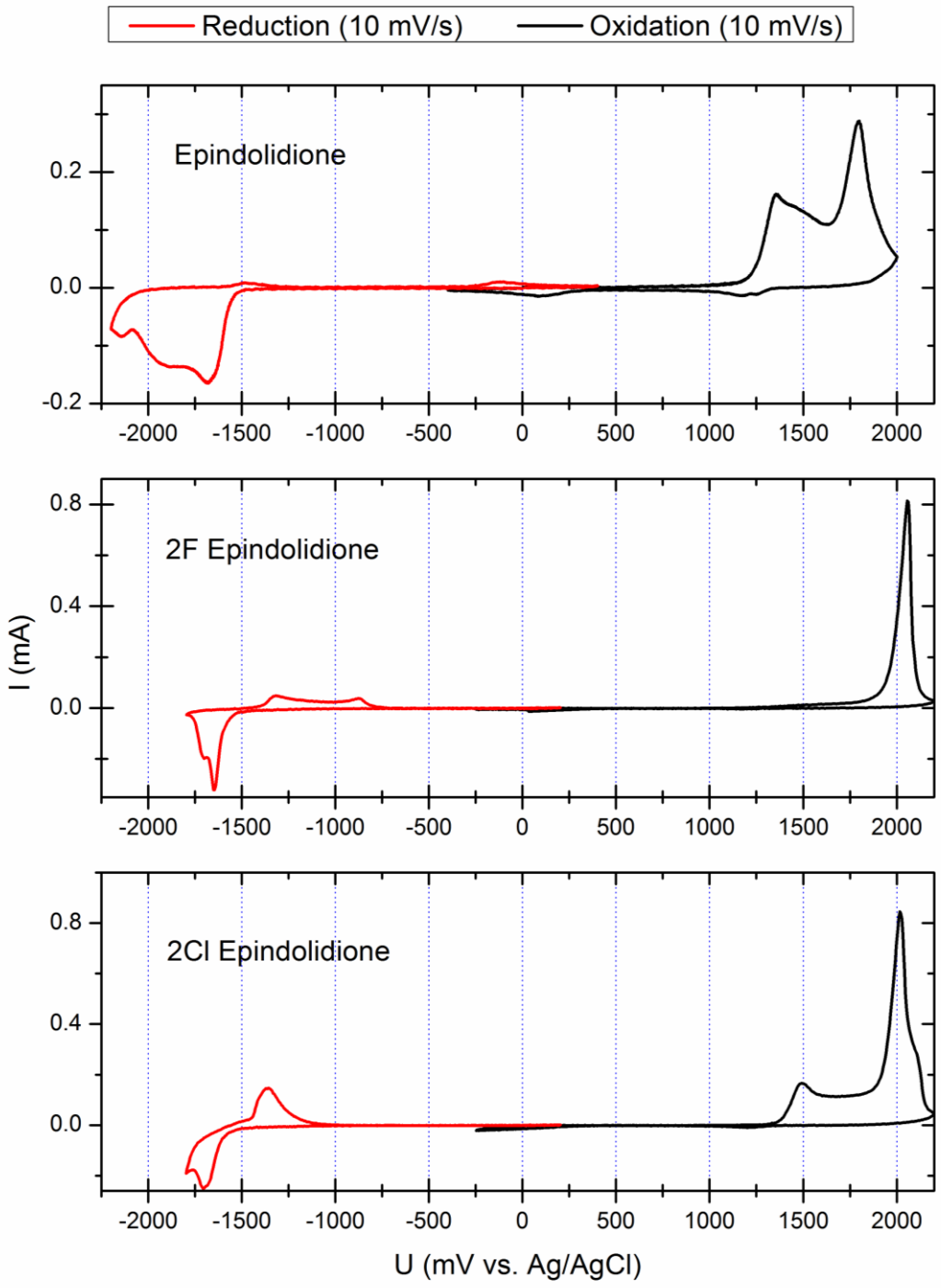

Figure 7. Cyclic voltammetry scans of thin films of different epindolidiones deposited on ITO functioning as the working electrode.

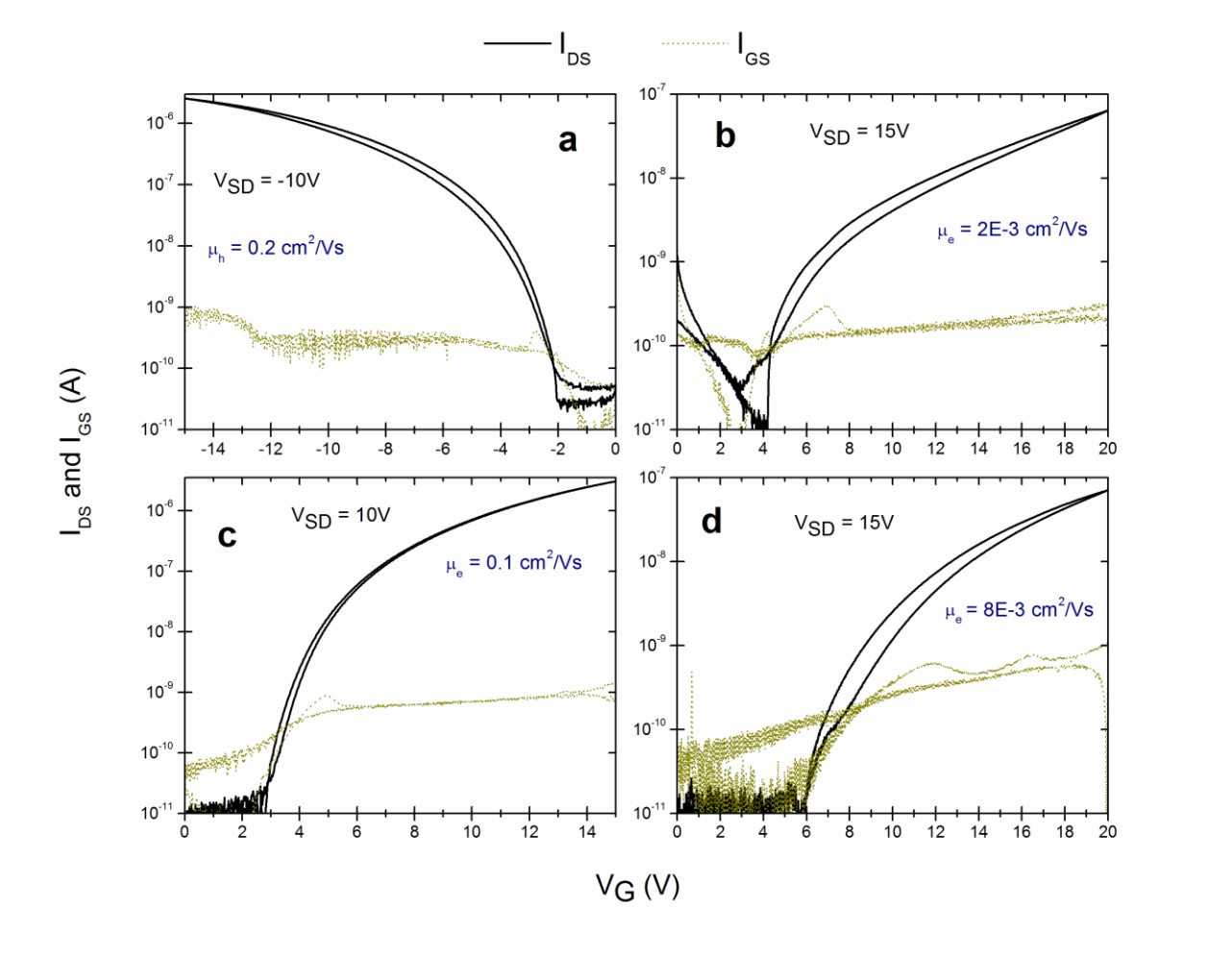

Figure 8. OFET transfer characteristics for a) Epi p-channel with Au source-drain electrodes, b) Epi n-channel with Al source-drain electrodes c) 2F-Epi n-channel with Al electrodes and d) 2Cl-Epi n-channel with Al source-drain electrodes.

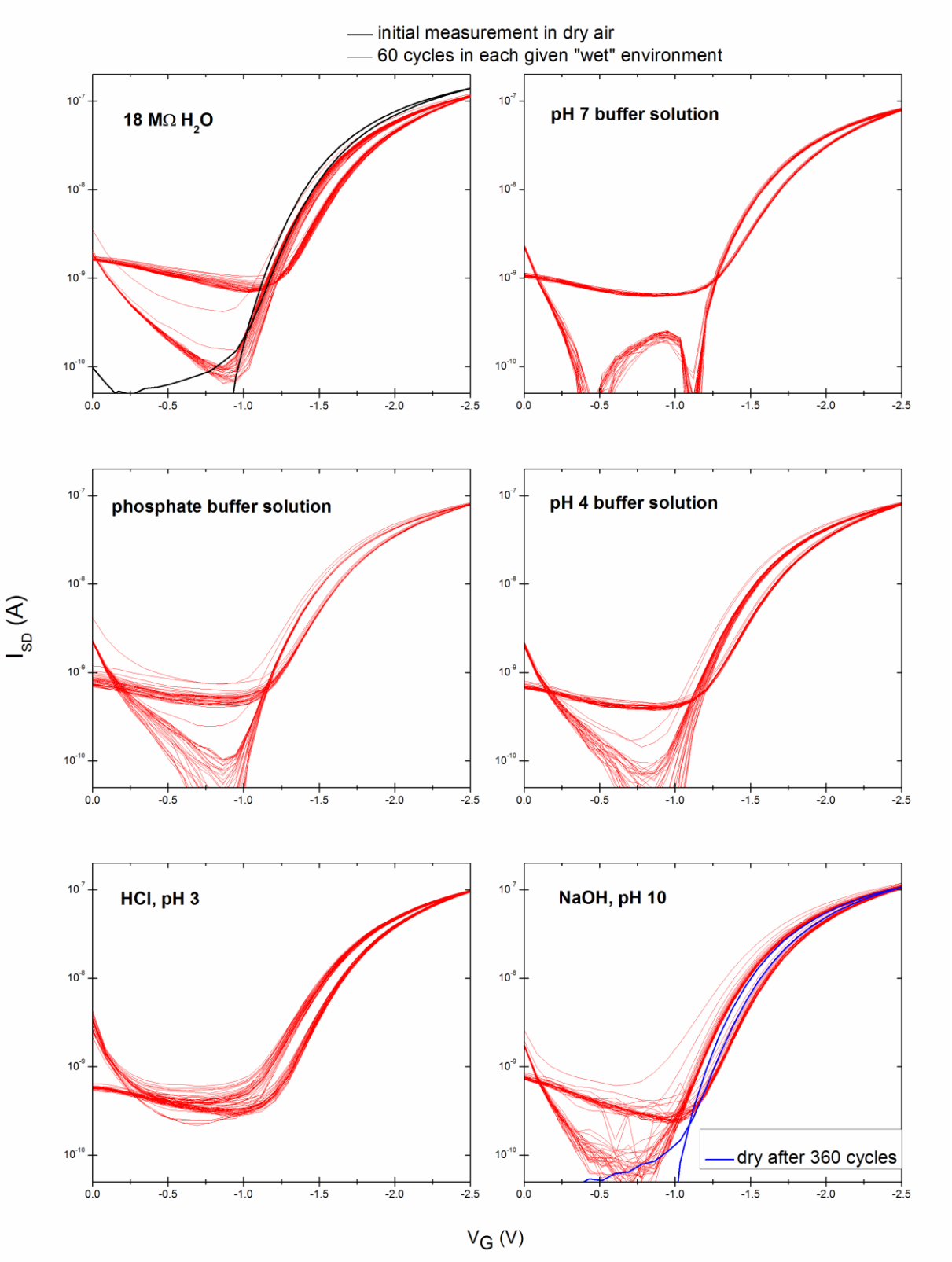

Figure 9. Low-voltage Epi transistor measured in air (black curve) and then 360 cycles in six different aqueous environments successively, with 60 cycles carried out in each. V_{SD} = - 0.5 V. Samples were rinsed with deionized water between different electrolytes.

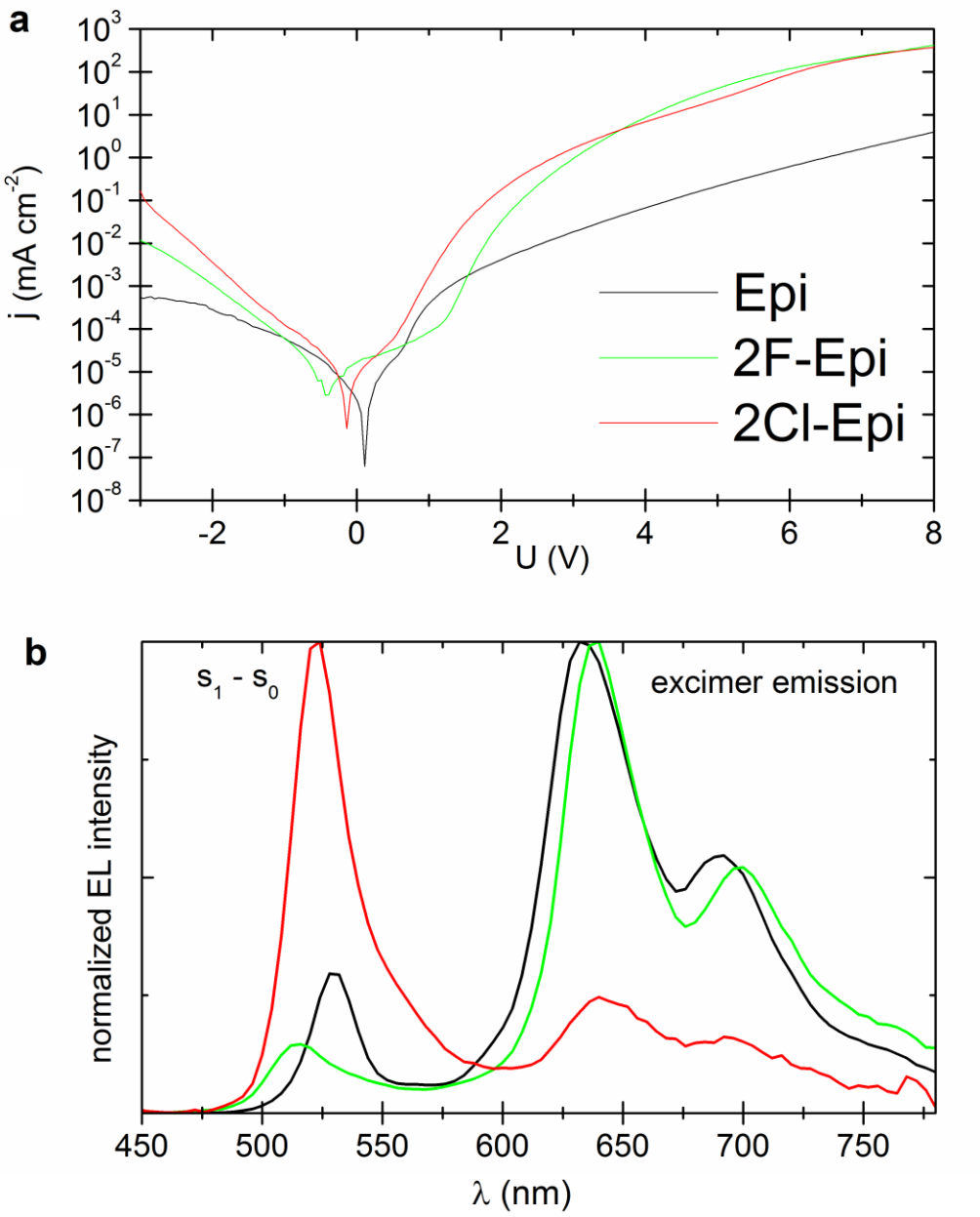

Figure 10. a) J-V characteristics of ITO/PEDOT:PSS/(Epi derivative)/Al diodes. b) Electroluminescence spectra of the same diodes operated in forward bias. Both the S_1-S_0 transition emitting green light and the excimers emitting yellow/red light can be observed.

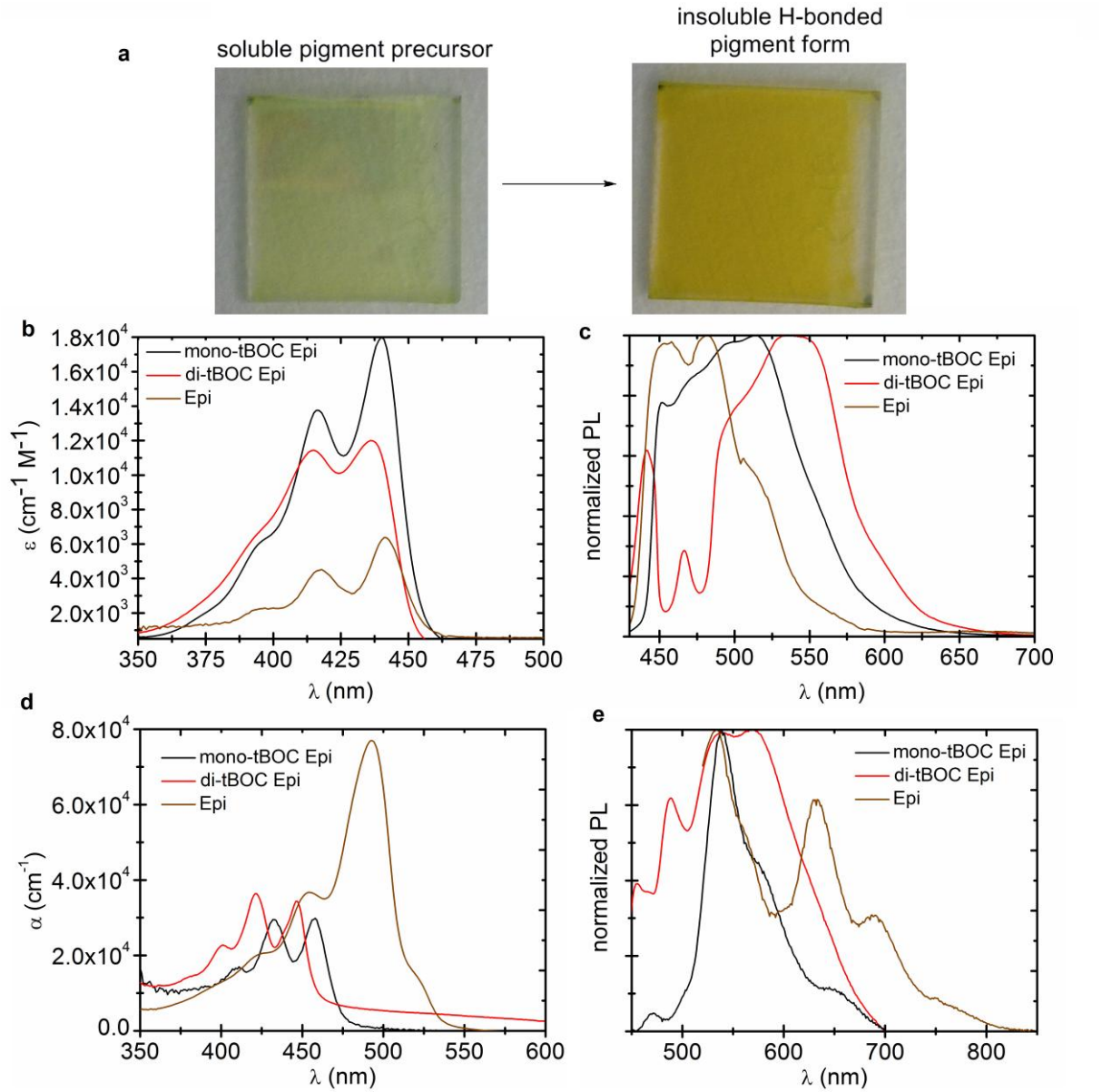

Figure 11. a) A spin-coated film on ITO-glass of di-tBOC Epi before and after thermal conversion into Epi. b) Comparison of extinction coefficients of Epi, mono-tBOC Epi, and di-tBOC-Epi in dilute chloroform solution. c) photoluminescence of the same chloroform solutions. d) Absorbance of thin films of mono-tBOC Epi, di-tBOC Epi, and Epi after thermal conversion deposited on fused silica. e) Photoluminescence spectra of the same films.

TOC:

Epindolidiones are H-bonded organic pigment semiconductors with excellent operational stability, including in aqueous media. We report on their crystal structure, electrochemical properties, and photophysics, which are dominated by excimeric effects. Transistor and light-emitting devices are demonstrated. We explore routes for solution processing of epindolidiones using transient solubilizing groups.

Keywords: Hydrogen-bonded pigments, organic semiconductors, indigoids, organic field-effect transistors

E. D. Głowacki*, G. Romanazzi, C. Yumusak, H. Coskun, U. Monkowius, G. Voss, M. Burian, R. T. Lechner, N. Demetri, G. J. Redhammer, N. Sünger, G. P. Suranna, N. S. Sariciftci

Epindolidiones – versatile and stable hydrogen-bonded pigments for organic field-effect transistors and light-emitting diodes

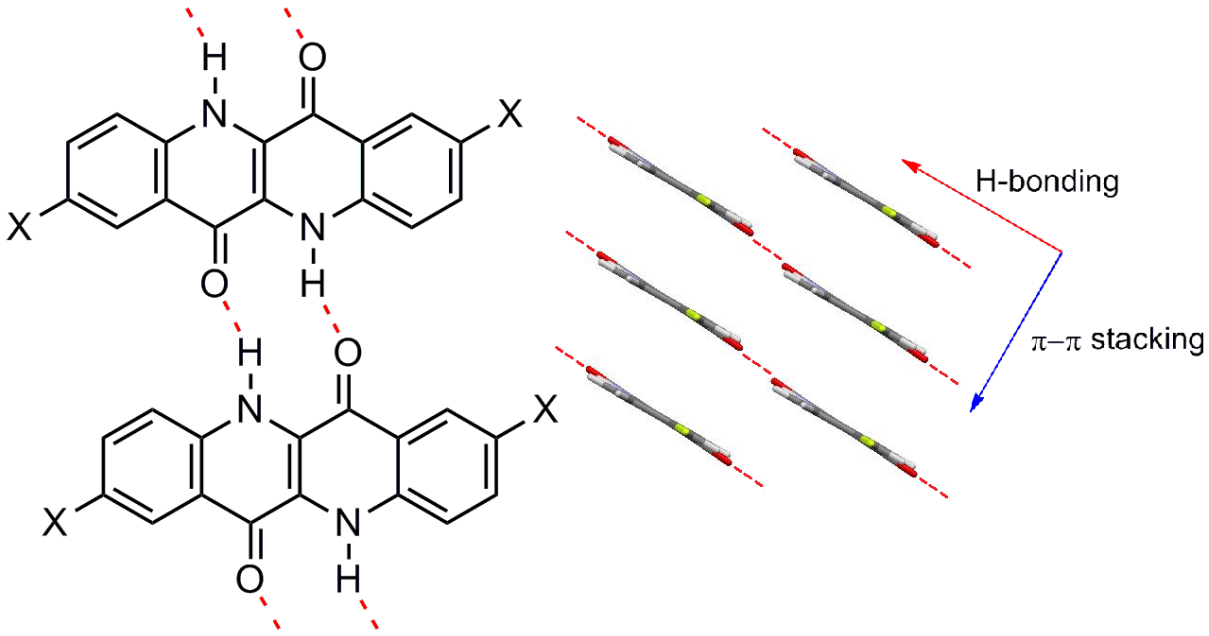

Supporting Information

Epindolidiones – versatile and stable hydrogen-bonded pigments for organic field-effect transistors and light-emitting diodes

E. D. Głowacki, G. Romanazzi, C. Yumusak, H. Coskun, U. Monkowius, G. Voss, M. Burian, R. T. Lechner, N. Demetri, G. J. Redhammer, N. Sünger, G. P. Suranna, N. S. Sariciftci*

Materials and synthetic methods

Reactants were purchased from Sigma-Aldrich® and used without further purification. All manipulations were carried out under inert nitrogen atmosphere using standard Schlenk techniques unless otherwise specified. All solvents used were carefully dried and freshly distilled according to standard laboratory practice. Flash column chromatography was performed using Merck® Kieselgel 60 (230–400 mesh) silica gel. ^{1}H NMR,^{13}C{^{1}H} NMR and ^{19}F NMR spectra were recorded on a Bruker Avance III 700 MHz or Bruker Avance 400 MHz and are reported in ppm relative to tetramethylsilane. FT-IR spectra (in KBr pellets) were recorded on a Jasco FT/IR 4200 spectrophotometer. Melting points were determined on a Büchi B-545 melting point apparatus and are uncorrected. Elemental analyses were obtained on a EuroVector CHNS EA3000 elemental analyser using acetanilide as analytical standard material. The high resolution mass spectrometry (HRMS) analysis was performed using a Bruker microTOF Q II mass spectrometer equipped with an electrospray ion source operated in positive ion mode. The sample solutions (CH_3OH) were introduced by continuous infusion with a syringe pump at a flow rate of 180 μL min^{-1}. The instrument was operated with end-plate offset and capillary voltages set to −500 V and −4500 V respectively. The nebulizer pressure was 0.4 bar (N_2), and the drying gas (N_2) flow rate was 4.0 L min^{-1}. The capillary exit and skimmer voltages were 90 V and 30 V respectively. The drying gas temperature was set at 180°C. The calibration was carried out with a sodium formate solution (10 mM NaOH in isopropanol/water 1:1 (+0.2% HCOOH)) and the software used for the simulations was

Bruker Daltonics DataAnalysis (version 4.0). Thermogravimetric analyses (TGA) were performed in a nitrogen flow (40 mL min^{-1}) with a Perkin-Elmer Pyris 6 TGA in the range from 30 to 800 °C with a heating rate of 10 °C min^{-1}. Triplicate TGA runs have been performed to ensure reproducibility.

Synthesis

Dimethyl Dihydroxyfumarate (**1**). To a solution of dihydroxyfumaric acid (13.26 g, 89.55 mmol) in anhydrous methanol (70 mL) kept under stirring at 0°C, thionyl chloride (13.4 mL, ~184 mmol) was slowly added dropwise within 15 min. Subsequently, the mixture was allowed to reach room temperature and kept under vigorous stirring for 4 days. The precipitation of an off-white solid was observed. The solid was collected on a sintered glass filter (G4) and was washed with cold methanol (20 mL) then with water (80 mL) and eventually dried under vacuum at 60°C to afford **1** (12.87 g, 81.6 %) as a white solid. mp= 175−180°C (lit.[1] 168−172°C, lit.[2] 177−179°C, lit.[3] 165−173°C). ^{1}H NMR (700 MHz, $CDCl_3$, δ): 9.43 (s, 2H), 3.89 (s, 6H). $^{13}C\{^{1}H\}$ NMR (176 MHz, $CDCl_3$, δ): 168.04, 135.19, 53.15. IR (KBr) ν= 3376, 3178, 3013, 2962, 2850, 1670, 1460, 1443, 1399, 1252, 1023, 880, 774, 709, 693, 551 cm^{-1}. HRMS (ESI) *m*/*z*: $[M + Na]^+$ calcd for $C_6H_8O_6Na$, 199.0213; found, 199.0219 (−2.9 ppm). Anal. calcd for $C_6H_8O_6$: C 40.92, H 4.58; found: C 40.80, H 4.61.

[1] E. E. Jaffe, H. Matrick, *J. Org. Chem.* **1968**, *33*, 4004−4010.

[2] D. S. Kemp, B. R. Bowen, C. C. Muendel, *J. Org. Chem.* **1990**, *55*, 4650−4657.

[3] S. Goodwin, B. Witkop, *J. Amer. Chem. Soc.* **1954**, *76*, 5599−5603 and the reference therein.

Dimethyl 2,3-bis(phenylamino)maleate (**2a**). 0.65 mL (~7.8 mmol) of concentrated HCl were added to a mixture of **1** (11.10 g, 63.0 mmol) and aniline (12.96 g, 139.2 mmol) in methanol (50 mL). The mixture was stirred under reflux. About 1 h was required for complete solubilisation, and shortly afterwards the precipitation of a yellowish-white solid was observed. After 5 h the reaction mixture was slowly cooled to room temperature and then filtered through a sintered glass filter (G4). The collected solid was washed with cold methanol (3x150 mL) and then dried under vacuum at 60°C to afford **2a** (18.02 g, 86.6 %) as white solid. mp=189.3±0.7°C (lit.[1] 196−198°C, lit.[4] 172°C). ^{1}H NMR (700 MHz, $CDCl_3$, δ): 7.25-7.22 (m, 4H), 6.98-6.95 (m, 2H), 6.87 (d, J=8.4 Hz, 4H), 5.85 (s, 2H), 3.76 (s, 6H). $^{13}C\{^{1}H\}$ NMR (176 MHz, $CDCl_3$, δ): 165.21, 141.81, 129.34, 125.11, 122.34, 117.80. 52.36. IR (KBr) ν= 3340, 3289, 3042, 3019, 2989, 2946, 1732, 1681, 1591, 1572, 1500, 1474, 1439, 1424, 1381, 1332, 1286, 1242, 1224, 1193, 1173, 1144, 1036, 958, 794, 750, 707, 695 cm^{-1}. HRMS (ESI) *m/z*: $[M + Na]^+$calcd for $C_{18}H_{18}N_2O_4Na$, 349.1159; found, 349.1153 (+1.8 ppm). Anal. calcd for $C_{18}H_{18}N_2O_4$: C, 66.25; H, 5.56; N, 8.58; found: C 65.95, H 5.60, N, 8.53.

Dimethyl 2,3-bis((4-fluorophenyl)amino)maleate (**2b**). The synthesis of **2b** was carried out by the following the procedure reported for **2a** using 1.775 g (10.08 mmol) of **1**, 2.650 g (23.85 mmol) of 4-fluoroaniline, 110 μL (~ 1.3 mmol) of concentrated HCl and 11 mL of methanol respectively. The product **2b** (3.273 g, 89.6 %) was isolated as white solid. mp=199.4±1.7°C (lit.[1] 196−198°C). ^{1}H NMR (700 MHz, $CDCl_3$, δ): 6.96-6.92 (m, 4H); 6.85-6.81(m, 4H); 5.76 (s, 2H); 3.74 (s, 6H). ^{19}F NMR (376 MHz, $CDCl_3$, δ): −120.87 (m, 2F). IR (KBr) ν=3330, 3275, 3087, 3062, 3037, 2988, 2951, 1733, 1678, 1604, 1574, 1501, 1484, 1464, 1435, 1400, 1380, 1336, 1287, 1212, 1144, 1092, 1034, 956, 853, 831, 820, 780, 749, 712,

[4] A. Salmony, H. Simonis, *Chem. Ber.* **1905**, *38*, 2580−2601.

664, 641, 559, 526 cm^{-1}. HRMS (ESI) *m/z*: $[M + Na]^+$ calcd for $C_{18}H_{16}F_2N_2O_4Na$, 385.0970; found, 385.0982 (−1.7 ppm). Anal. calcd for $C_{18}H_{16}F_2N_2O_4$: C, 59.67; H, 4.45; N, 7.73; found: C 59.36, H 4.41, N, 7.60.

Dimethyl 2,3-bis((4-chlorophenyl)amino)maleate (**2c**). The synthesis of **2c** was carried out following the procedure reported for **2a** using 1.756 g (9.97 mmol) of **1**, 2.905 g (22.77 mmol) of 4-chloroaniline, 100 μL (~ 1.2 mmol) of concentrated HCl and 10 mL of methanol respectively. The product **2c** (3.400 g, 86.5 %) was isolated as yellowish-white solid. mp=206.5±0.2°C (lit.[1] 203−204°C). ^{1}H NMR (700 MHz, $CDCl_3$, δ): 7.21-7.18 (m, 4H), 6.80-6.74 (m, 4H), 5.78 (s, 2H), 3.76 (s, 6H). $^{13}C\{^1H\}$ NMR (176 MHz, $CDCl_3$, δ):164.88; 140.16; 129.37; 127.67; 124.97; 119.11; 52.53. IR (KBr) ν=3328, 3273, 3023, 2990, 2946, 2846, 1732, 1679, 1590, 1572, 1493, 1438, 1332, 1239, 1225, 1192, 1146, 1095, 1035, 1013, 958, 852, 821, 798, 767, 755, 715, 672, 652, 637, 609, 545 cm^{-1}. HRMS (ESI) *m/z*: $[M + Na]^+$ calcd for $C_{18}H_{16}Cl_2N_2O_4Na$, 417.0379; found, 417.0367 (+2.5 ppm). Anal. calcd for $C_{18}H_{16}Cl_2N_2O_4$ C, 54.70; H, 4.08; N, 7.09; found: C 54.37, H 4.02, N, 7.20.

2-Methoxycarbonyl-3-phenylamino-4-quinolone (**3a**). In a 1-L round-bottom flask equipped with a Dean-Stark apparatus, a mixture of Dowtherm™ A [5] (260 mL) and **2** (16.15 g, 49.49 mmol) was vigorously stirred and heated to reflux (approx. 255-260°C) within 30 min. The reaction was prolonged for further 30 min, subsequently slowly cooled to room temperature and decanted for 18 h. The precipitation of a brownish-yellow solid product was observed. The solid was collected on a sintered glass filter (G4), and washed (3x100 mL) with

[5] DOWTHERM™ A heat transfer fluid is a eutectic mixture of two very stable compounds, biphenyl (26.5%$_W$) and diphenyl oxide (73.5%$_W$). These compounds have practically the same vapor pressures, so the mixture can be handled as if it were a single compound.

petroleum ether (bp 40-60°C). Eventually, the solid was dried under vacuum at 60°C affording **3a** (9.42 g, 79.4 %) as yellow powder. mp=207.2±0.2°C (lit.[1] 201.5−203°C). ^{1}H NMR (700 MHz, DMSO-d_6, δ): 11.84 (br s, 1H); 8.12 (ddd, J=8.2, 1.5, 0.45 Hz, 1H), 7.86-7.84 (m, 1H), 7.62 (ddd, J=8.6, 6.7, 1.5 Hz, 1H), 7.46 (s, 1H), 7.33-7.30 (m, 1H), 7.12-7.09 (m, 2H), 6.74-6.70 (m, 3H), 3.68 (s, 3H). ^{13}C{^{1}H} NMR (176 MHz, DMSO-d_6, δ): 173.60, 163.45, 145.54, 138.44, 131.85, 129.10, 128.37, 125.21, 124.93, 123.02, 122.79, 118.99, 118.67, 115.36, 52.64. IR (KBr) ν= 3376, 3072, 2950, 1735, 1710, 1624, 1603, 1560, 1525, 1498, 1476, 1450, 1440, 1384, 1362, 1325, 1304, 1267, 1227, 1174, 965, 770, 756, 697, 532 cm^{-1}. HRMS (ESI) *m*/*z*: [M + Na]$^{+}$calcd for $C_{17}H_{14}N_2O_3Na$, 317.0897; found, 317.0902 (−1.5 ppm). Anal. calcd for $C_{17}H_{14}N_2O_3$: C, 69.38; H, 4.79; N, 9.52; found: C 69.02, H 4.83, N, 9.46.

2-Methoxycarbonyl-3-((4-fluorophenyl)amino)-6-fluoro-4-quinolone (**3b**). The synthesis of **3b** was carried out following the procedure reported for **3a** using 2.920 g (8.06 mmol) of **2b** and 44 mL of Dowtherm™ A respectively. The product **3b** (2.314 g, 86.9 %) was isolated as yellow solid. mp=224.6±1.0°C (lit.[1] 223−226°C). ^{1}H NMR (700 MHz, DMSO-d_6, δ): 12.01 (s, 1H); 7.94 (dd, J=9.3, 4.7 Hz, 1H); 7.74 (dd, J=9.3, 3.0 Hz, 1H); 7.62-7.59 (m, 1H); 7.51 (s, 1H); 6.96-6.92 (m, 2H); 6.71 (dd, J=8.9, 4.7 Hz, 2H); 3.71 (s, 3H). ^{19}F NMR (376 MHz, DMSO-d_6, δ): −117.95 (br m, 1F); −125.66 (br m, 1F). IR (KBr) ν=3328, 3237, 3004, 2952, 1711, 1565, 1546, 1508, 1484, 1435, 1409, 1358, 1292, 1272, 1226, 1155, 958, 833, 809, 771, 739, 698, 564, 529 cm^{-1}. HRMS (ESI) *m*/*z*: [M + Na]$^{+}$calcd for $C_{17}H_{12}F_2N_2O_3Na$, 353.0708; found, 353.0701 (+2.1 ppm). Anal. calcd for $C_{17}H_{12}F_2N_2O_3$: C, 61.82; H, 3.66; N, 8.48; found: C 61.63, H 3.63, N, 8.40.

2-Methoxycarbonyl-3-((4-clorophenyl)amino)-6-cloro-4-quinolone (**3c**). The synthesis of **3c** was carried out following the procedure reported for **3a** using 3.121 g (7.89 mmol) of **2c** and 40 mL of Dowtherm™ A respectively. The product **3c** (2.530 g, 88.2 %) was isolated as yellow solid. mp=258.4±0.7°C (lit.[1] 247−248.5°C). ^{1}H NMR (700 MHz, DMSO-d_6, δ): 12.10 (s, 1H); 8.04 (d, J=2.5 Hz, 1H); 7.90 (d, J=9.0 Hz, 1H); 7.72 (dd, J=9.0, 2.5 Hz, 1H); 7.70 (s, 1H); 7.13-7.10 (m, 2H); 6.70-6.67 (m, 2H); 3.75 (s, 3H). ^{13}C{^{1}H} NMR (101 MHz, DMSO-d_6, δ): 172.51; 163.42, 144.66; 137.33; 132.30; 128.21; 127.87; 124.96; 124.46; 123.89; 121.94; 121.90; 116.84; 53.14. IR (KBr) ν= 3338, 3226, 2948, 1713, 1565, 1493, 1469, 1438, 1404, 1358, 1296, 1270, 1243, 1217, 1174, 1093, 1071, 977, 946, 842, 822, 773, 760, 710, 663, 540, 520 cm^{-1}. HRMS (ESI) *m/z*: [M + Na]$^{+}$calcd for $C_{17}H_{12}Cl_2N_2O_3Na$, 385.0117; found, 385.0105 (+3.2 ppm). Anal. calcd for $C_{17}H_{12}Cl_2N_2O_3$: C, 56.22; H, 3.33; Cl, 19.52; N, 7.71; found: C 55.82, H 3.36, N, 7.60.

Dibenzo[b,g][1,5]naphthyridine-6,12(5H,11H)-dione (**Epi**)**.** A mixture of 83.2 g of polyphosphoric acid $H_{2+n}P_nO_{3n+1}$ (115% H_3PO_4 basis) and **3a** (8.320 g, 28.27 mmol) was heated at 150°C for 3.5 h under stirring. The mixture was then cooled to ~50°C and then water (700 mL) was slowly added, keeping the temperature constant until the exothermic process ceased. The reaction mixture was filtered through a sintered glass filter (G4) and the collected solid was washed several times with water (7x150 mL) until free of acid and subsequently with cold methanol (3x150 mL). Eventually, the solid was dried under vacuum at 80°C affording **Epi** (6.59 g, 88.9 %) as a greenish-yellow powder. mp >400°C. ^{1}H NMR (700 MHz, DMSO-d_6, δ): 11.92 (br s, 2H); 8.29 (ddd, J=8.2, 1.5, 0.45 Hz, 2H), 8.09 (ddd, J=8.6, 1.1, 0.65 Hz, 2H), 7.76 (ddd, J=8.6, 6.7, 1.5 Hz, 2H), 7.33 (ddd, J=8.2, 6.7, 1.1 Hz, 2H). IR (KBr) ν= 3216, 3189, 3163, 3126, 2954, 1627, 1583, 1564, 1517, 1469, 1423, 1381, 1370,

1328, 1297, 1245, 1100, 1025, 937, 801, 744, 700, 531 cm^{-1}. Anal. calcd for $C_{16}H_{10}N_2O_2$: C, 73.27; H, 3.84; N, 10.68; found: C, 73.67; H, 3.87; N, 10.74.

2,8-difluorodibenzo[b,g][1,5]naphthyridine-6,12(5H,11H)-dione (**2F-Epi**). The synthesis of **2F-Epi** was carried out following the procedure reported for **Epi** using 2.146 g (6.50 mmol) of **3b** and 21.5 g of polyphosphoric acid $H_{2+n}P_nO_{3n+1}$ (115% H_3PO_4 basis) respectively. The product **2F-Epi** (1.782 g, 92.0 %) was isolated as yellow solid. mp >400°C. ^{1}H NMR (700 MHz, D_2SO_4, δ): 8.71-8.65 (m, 2H); 8.50-8.45 (m, 2H); 8.41-8.35 (m, 2H). ^{19}F NMR (376 MHz, D_2SO_4, δ): −109.20 (br m, 2F). IR (KBr) ν= 3204, 3170, 3096, 2994, 1589, 1571, 1561, 1520, 1481, 1387, 1308, 1242, 1212, 1084, 975, 868, 822, 725, 659, 568, 538 cm^{-1}. Anal. calcd for $C_{16}H_8F_2N_2O_2$: C, 64.43; H, 2.70; N, 9.39; found: C, 64.23; H, 2.69; N, 9.36.

2,8-dichlorodibenzo[b,g][1,5]naphthyridine-6,12(5H,11H)-dione (**2Cl-Epi**). The synthesis of **2Cl-Epi** was carried out following the procedure reported for **Epi** using 2.340 g (6.44 mmol) of **3c** and 23.4 g of polyphosphoric acid $H_{2+n}P_nO_{3n+1}$ (115% H_3PO_4 basis) respectively. The product **2Cl-Epi** (2.092 g, 98.1 %) was isolated as yellow solid. mp >400°C. ^{1}H NMR (700 MHz, D_2SO_4, δ):8.81 (s, 2H); 8.58-8.52 (m, 2H); 8.50-8.44 (m, 2H). IR (KBr) ν= 3208, 3180, 3115, 3076, 3012, 1616, 1581, 1557, 1505, 1462, 1371, 1303, 1233, 1182, 1140, 1114, 1071, 952, 886, 821, 735, 702, 642, 557, 528 cm^{-1}. Anal. calcd for $C_{16}H_8Cl_2N_2O_2$: C, 58.03; H, 2.43; N, 8.46; found: C, 57.74; H, 2.45; N, 10.65.

Di-tert-butyl 6,12-dioxodibenzo[b,g][1,5]naphthyridine-5,11(6H,12H)-dicarboxylate (**di-tBOC-Epi**) *and tert-butyl 6,12-dioxo-11,12-dihydrodibenzo[b,g][1,5]naphthyridine-5(6H)-carboxylate* (**mono-tBOC-Epi**). A mixture of epindolidione (**Epi**, 790 mg, 3.01 mmol), 4-dimethylaminopyridine (DMAP, 736 mg, 6.0 mmol) in dry THF (75 mL) was stirred at room

temperature. After 15 min, di-*tert*-butyl dicarbonate ($(tBOC)_2O$, 10.53 g, 48.25 mmol) was added in one portion. The mixture was stirred at 40°C for 96 h and monitored by thin layer chromatography (TLC). The mixture was then filtrated, and the solid recovered (unreacted **Epi**, 216 mg). The filtrate was concentrated in *vacuo* to remove solvent and excess of $tBOC_2O$ at 45°C. The crude residue was purified by flash column chromatography on silica gel using dichloromethane (R_f=0.33) as eluent to afford **di-tBOC-Epi** (488 mg, 35 %) as yellow solid and then dichloromethane/ethyl acetate (92:08=v:v, R_f=0.42) as eluent to afford **mono-tBOC-Epi** (174.5 mg, 16 %) as yellow solid. **di-tBOC-Epi**: ^{1}H NMR (700 MHz, $CDCl_3$, δ): 8.45 (dd, J=8.1, 1.6 Hz, 2H); 7.90 (d, J=8.7 Hz, 2H); 7.76 (ddd, J=8.6, 7.0, 1.6 Hz, 2H); 7.43-7.40 (m, 2H), 1.69 (s, 18H). $^{13}C\{^1H\}$ NMR (176 MHz, $CDCl_3$, δ): 173.27; 150.66; 138.40; 134.36 ; 126.94; 123.69, 122.71; 116.17; 86.40; 27.59. IR (KBr) ν= 3007, 2988, 2935, 1760, 1630, 1608, 1573, 1478, 1393, 1363, 1347, 1308, 1260, 1238, 1222, 1153, 1124, 1108, 1035, 990, 895, 843,781, 745, 695, 572, 557 cm^{-1}. HRMS (ESI) *m*/*z*: $[M + Na]^+$calcd for $C_{26}H_{26}N_2O_6Na$, 485.1683; found, 485.1680 (+0.9 ppm). Anal. calcd for $C_{26}H_{26}N_2O_6$: C, 67.52; H, 5.67; N, 6.06; found: C, 67.37; H, 5.64; N, 6.03. **mono-tBOC-Epi**: ^{1}H NMR (700 MHz, DMSO-d_6, δ): 12.20 (br s, 1H); 8.39 (dd, J=8.1, 1.6 Hz, 1H); 8.22 (dd, J=8.1, 1.3 Hz, 1H); 8.09-8.04 (m, 1H); 7.94-7.89 (m, 1H); 7.80 (d, J=8.7 Hz 1H); 7.78-7.74 (m, 1H); 7.50-7.45 (m, 1H); 7.38-7.32 (m, 1H); 1.64 (s, 9H). IR (KBr) ν= 3249, 3168, 3010, 2977, 2935, 1758, 1618, 1604, 1578, 1490, 1399, 1369, 1335, 1311, 1242, 1222, 1152, 1126, 1104, 1024, 1003, 983, 841, 753, 742, 697, 547 cm^{-1}. HRMS (ESI) *m*/*z*: $[M + Na]^+$calcd for $C_{21}H_{18}N_2O_4Na$, 385.1159; found, 385.1163 (−0.7 ppm). Anal. calcd for $C_{21}H_{18}N_2O_4$: C, 69.60; H, 5.01; N, 7.73; found: C 69.31, H 5.04, N, 7.62.

Crystal Structure Determination

Single-crystal structure analysis of 2Cl-Epi was carried out on a Bruker Smart APEX diffractometer operating with Mo-Kα radiation (λ= 0.71073 Å). The structures were solved by

direct methods (SHELXS-97) and refined by full-matrix least squares on F2 (SHELXL-97).[6] The H atoms were calculated geometrically, and a riding model was applied in the refinement process.

For 2F-Epi, data collections were performed at the X-ray diffraction beamline (XRD1) of the Elettra Synchrotron, Trieste (Italy). Complete datasets were collected at 100 K (nitrogen stream supplied through an Oxford Cryostream 700) with a monochromatic wavelength of 0.700 Å through the rotating crystal method. Images were acquired using a Pilatus 2M image plate detector. The crystals of compound 2F-Epi were dipped in N-paratone and mounted on the goniometer head with a nylon loop. The diffraction data were indexed, integrated and scaled using XDS.[1S] The compound crystallize with a triclinic unit cell. Complete datasets were obtained by merging two data collections obtained from two crystals mounted with different orientations. The unit cell and space group have also been determined at room temperature and no phase change has been detected. The structures were solved by direct methods using SIR2014,[2S] Fourier analyzed and refined by the full-matrix least-squares based on F^2 implemented in SHELXL-2014.[3S] The Coot program was used for modeling.[4S] Anisotropic thermal motion modeling was then applied to atoms with full occupancy. Hydrogen atoms were included (except for disordered water molecules) at calculated positions with isotropic $U_{factors} = 1.2\ U_{eq}$.

The 2X-Epi molecules show an inversion center which is located on an inversion center of the triclinic *P*-1 cell. The asymmetric units therefore contains half 2X-Epi molecule only. No disorder and no solvent molecules are present in this crystal form.

	2F-Epi	**2Cl-Epi**
Moiety Formula	$C_{16}H_8F_2N_2O_2$	$C_{16}H_8Cl_2N_2O_2$
Empirical Formula	$C_{16}H_8F_2N_2O_2$	$C_{16}H_8Cl_2N_2O_2$
Formula weight (Da)	298.24	331.14
Temperature (K)	100(2)	298(2)
Wavelength (Å)	0.700	0.71073
Crystal system	triclinic	triclinic
Space Group	*P*-1	*P*-1
a (Å)	3.690(1)	3.900(3)
b (Å)	5.976(1)	6.260(5)
c (Å)	13.489(2)	13.593(12)
α (°)	101.785(2)	90.947(11)
β (°)	94.892(6)	96.272(10)
γ (°)	92.309(10)	98.599(9)
V ($Å^3$)	289.61(10)	326.0(5)
Z	1	1

[6] G. M. Sheldrick, *SHELXS-97, Program for the Solution of Crystal Structures*, Göttingen, Germany, 1997. See also: G. M. Sheldrick, *Acta Crystallographica*, 1990, **A46**, 467-473

ρ (g·cm^{-3})	1.710	1.687
F(000)	152.0	168
μ (mm^{-1})	0.130	0.51
θ min,max (°)	1.5, 27.8	3.0, 24.0
Resolution (Å)	0.75	0.87
Total refl. collctd	7580	1950
Independent refl.	1412	1022
Obs. Refl. [Fo>4σ(Fo)]	1324	547
I/σ(I) (all data)	21.87	-
I/σ(I) (max resltn)	17.67	-
Completeness (all data)	0.99	0.99
Completeness (max resltn)	0.96	-
Rmerge (all data)	0.062	-
Rmerge (max resltn,)	0.066	-
Multiplicity (all data)	5.4	-
Multiplicity (max resltn)	5	-
Data/restraint/parameters	1397/0/101	1022/0/100
Goof	1.045	0.940
R[I>2.0σ(I)], wR2 [I>2.0σ(I)]	0.0371, 0. 1078	0.058, 0.129
R (all data), wR2 (all data)	0.0385, 0.1102	0.1295, 0.1289
CCDC number	1013233	1013474

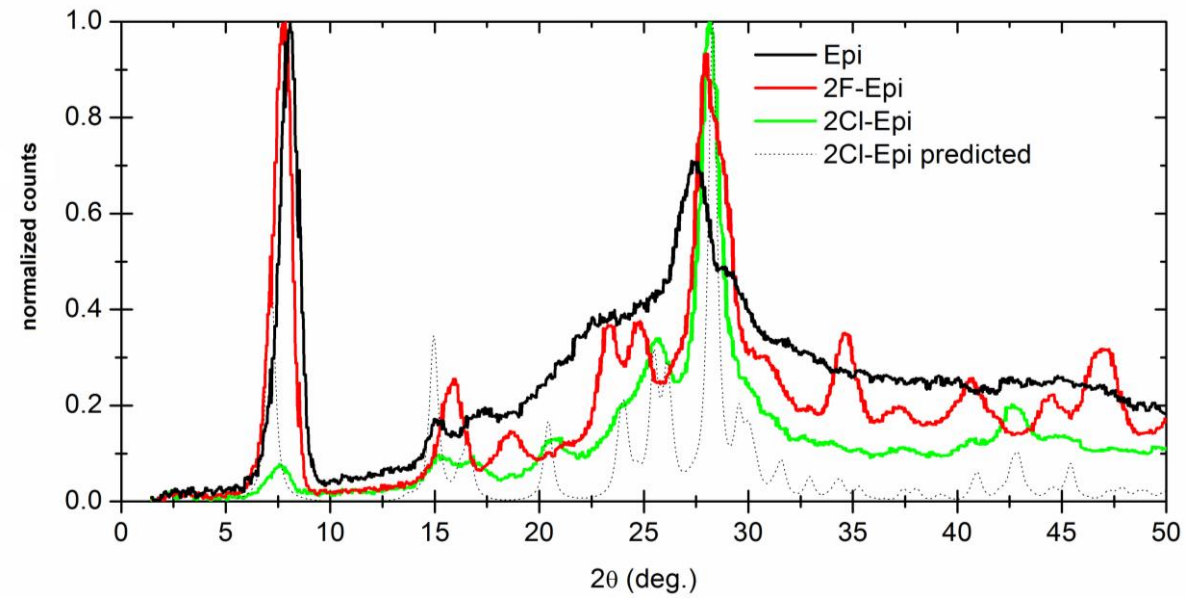

Figure S1. X-ray powder diffraction of the three derivatives, compared with the predicted powder spectrum of 2Cl-Epi calculated based on the X-ray single-crystal structure.

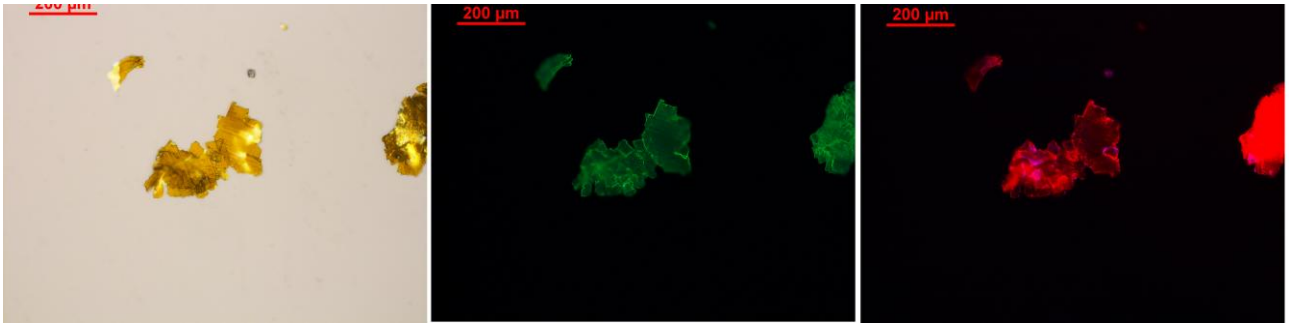

Figure S2. Photomicrographs of epindolidione crystals grown by sublimation. On the left is the episcopic-illuminated bright-field image. The central image is taken using a blue-excitation filter cube, while the right image is taken using a green-excitation filter cube. Both green and red emission can be seen emitting from all parts of the crystals.